

# Lecture 6) Multidimensional Schemes for Hyperbolic Conservation Laws: Bringing it Together

By

Prof. Dinshaw S. Balsara ([dbalsara@nd.edu](mailto:dbalsara@nd.edu))

Les Houches Summer School in Computational Astrophysics

<http://www.nd.edu/~dbalsara/Numerical-PDE-Course>



## 7.1) Introduction

This is the chapter where we bring together all our ideas on hyperbolic conservation laws.

Multi-d **conservation law**:  $U_t + F(U)_x + G(U)_y = 0$

Whether it is hyperbolic depends on **eigenstructure** of :

$$A \equiv \frac{\partial F(U)}{\partial U} = R \Lambda L \quad ; \quad B \equiv \frac{\partial G(U)}{\partial U}$$

Written in **conservation form**:

$$\bar{U}_{i,j}^{n+1} = \bar{U}_{i,j}^n - \frac{\Delta t}{\Delta x} \left( \bar{F}_{i+1/2,j}^{n+1/2} - \bar{F}_{i-1/2,j}^{n+1/2} \right) - \frac{\Delta t}{\Delta y} \left( \bar{G}_{i,j+1/2}^{n+1/2} - \bar{G}_{i,j-1/2}^{n+1/2} \right)$$

Question: What are the benefits of conservation form? Why do we have overbars?

Avoiding **spurious oscillations**: Non-linear hybridization; TVD  
Reconstruction

Hyperbolic conservation law becomes simple in **characteristic variables**:

$$w_t^m + \lambda^m w_x^m = 0 \quad \text{with} \quad w^m(x) = l^m U(x) \quad \forall \quad m = 1, \dots, M$$

Above equation still holds *locally*, though not *globally* when non-linearities are introduced.

**Riemann problem** is essential for dealing with **non-linearities**.

Various kinds of **approximate Riemann solvers** were studied.

We will always begin with examples of **second order** schemes. Then we will show how the methodology is extended **to higher order schemes**. I.e. go from the familiar to that which may be less familiar.

## 7.2) Reconstructing the Solution for Conservation Laws – Part I, TVD & PPM Reconstruction

### 7.2.1) TVD Reconstruction in Conserved, Primitive or Characteristic Variables

#### The Problem:

Let  $\mathbf{U}$  be an  $M$ -component solution vector for a 2D conservation law. At a time  $t^n$  in a zone  $(i,j)$ , we start with zone-averaged values. We wish to **reconstruct** the solution:

$$\mathbf{U}_{i,j}^n(\tilde{x}, \tilde{y}) = \bar{\mathbf{U}}_{i,j}^n + \Delta_x \bar{\mathbf{U}}_{i,j} \tilde{x} + \Delta_y \bar{\mathbf{U}}_{i,j} \tilde{y} \quad \text{where } \tilde{x} \equiv (x - x_i)/\Delta x ; \tilde{y} \equiv (y - y_j)/\Delta y$$

**Reconstruction** means we use the mesh function  $\{\bar{\mathbf{U}}_{i,j}^n\}$  to obtain  $\Delta_x \bar{\mathbf{U}}_{i,j}$  and  $\Delta_y \bar{\mathbf{U}}_{i,j}$  in each zone.

The Solution: Three ways to do it:

- A) Reconstruct on the *conserved variables*.
- B) Reconstruct on the *primitive variables*.
- C) Reconstruct on the *characteristic variables*.

A) Componentwise Reconstruction on the *conserved variables*:

Let  $\bar{u}_{i,j}^m$  be the  $m^{\text{th}}$  component of  $\bar{U}_{i,j}^n$ .

For each of the components, we want:

$$u_{i,j}^m(\tilde{x}, \tilde{y}) = \bar{u}_{i,j}^m + \Delta_x \bar{u}_{i,j}^m \tilde{x} + \Delta_y \bar{u}_{i,j}^m \tilde{y}$$

with:

$$\Delta_x \bar{u}_{i,j}^m = \text{Limiter} \left( \bar{u}_{i+1,j}^m - \bar{u}_{i,j}^m, \bar{u}_{i,j}^m - \bar{u}_{i-1,j}^m \right) \quad ;$$

$$\Delta_y \bar{u}_{i,j}^m = \text{Limiter} \left( \bar{u}_{i,j+1}^m - \bar{u}_{i,j}^m, \bar{u}_{i,j}^m - \bar{u}_{i,j-1}^m \right)$$

Question: What are the advantages and disadvantages of this form of limiting?

## B) Componentwise Reconstruction on the *primitive variables*:

From each vector  $\bar{U}_{i,j}^n$ , obtain a vector of primitive variables  $V_{i,j}^n$

Let  $v_{i,j}^m$  be the  $m^{\text{th}}$  component of  $V_{i,j}^n$ .

For each of the components, we want:

$$v_{i,j}^m(\tilde{x}, \tilde{y}) = v_{i,j}^m + \Delta_x v_{i,j}^m \tilde{x} + \Delta_y v_{i,j}^m \tilde{y}$$

with:

$$\Delta_x v_{i,j}^m = \text{Limiter} \left( v_{i+1,j}^m - v_{i,j}^m, v_{i,j}^m - v_{i-1,j}^m \right) \quad ;$$

$$\Delta_y v_{i,j}^m = \text{Limiter} \left( v_{i,j+1}^m - v_{i,j}^m, v_{i,j}^m - v_{i,j-1}^m \right)$$

Question: What are the advantages and disadvantages of this form of limiting?

## C) Reconstruction on the *characteristic variables*:

For a linear system,  $w_t^m + \lambda^m w_x^m = 0$  is valid all over. Not so for a non-linear system.

Question: Why?

When the eigenvalues and eigenvectors become solution-dependent, we only have a **local representation of the eigensystem** within each zone.

I.e.,  $\lambda^m(\bar{U}_{i,j}^n)$ ,  $l^m(\bar{U}_{i,j}^n)$  and  $r^m(\bar{U}_{i,j}^n)$  have become solution-dependent.

In simple words, the left eigenvectors in zone  $(i+1, j)$ , given by  $\{l^m(\bar{U}_{i+1,j}^n) : m = 1, \dots, M\}$ , will not be orthonormal with the right eigenvectors in zone  $(i, j)$ , given by  $\{r^m(\bar{U}_{i,j}^n) : m = 1, \dots, M\}$ . Consequently, each zone defines its own *local eigenspace*.

Advantage of this Limiting:-Different wave families may have different properties. Some may be linearly degenerate with the result that they don't self-steepen (think contact discontinuity in Euler flow). Others may be genuinely non-linear so that they do self-steepen (think sound waves in Euler flow). **Different wave families have to be treated differently.**

We can only **project** the solution from neighboring zones **into an eigenspace** that is **specific to the zone  $(i, j)$**  as follows:

First, obtain the characteristic variables from the neighboring zones and the current zone **(pay attention to the subscripts)**:-

$$w_{i,j;L}^m = l^m \left( \bar{U}_{i,j}^n \right) \cdot \bar{U}_{i-1,j}^n \quad ; \quad w_{i,j;C}^m = l^m \left( \bar{U}_{i,j}^n \right) \cdot \bar{U}_{i,j}^n \quad ; \quad w_{i,j;R}^m = l^m \left( \bar{U}_{i,j}^n \right) \cdot \bar{U}_{i+1,j}^n \quad \forall \quad m = 1, \dots, M$$

Second, limit the local characteristic variable:

$$\Delta w_{i,j}^m = \text{Limiter} \left( w_{i,j;R}^m - w_{i,j;C}^m, w_{i,j;C}^m - w_{i,j;L}^m \right) \quad \forall \quad m = 1, \dots, M$$

Third, project the variation in the characteristic variables into the local space of right eigenvectors:

$$\Delta_x \bar{U}_{i,j} = \sum_{m=1}^M \Delta w_{i,j}^m \quad r^m \left( \bar{U}_{i,j}^n \right)$$

Question: What do subscripts “L”, “C” and “R” stand for? What are the advantages and disadvantages of this form of limiting?

Results from piecewise linear limiting. **Advect Gaussian, square wave, triangle and ellipse.** See if shape is preserved. But what is that scheme to the right?

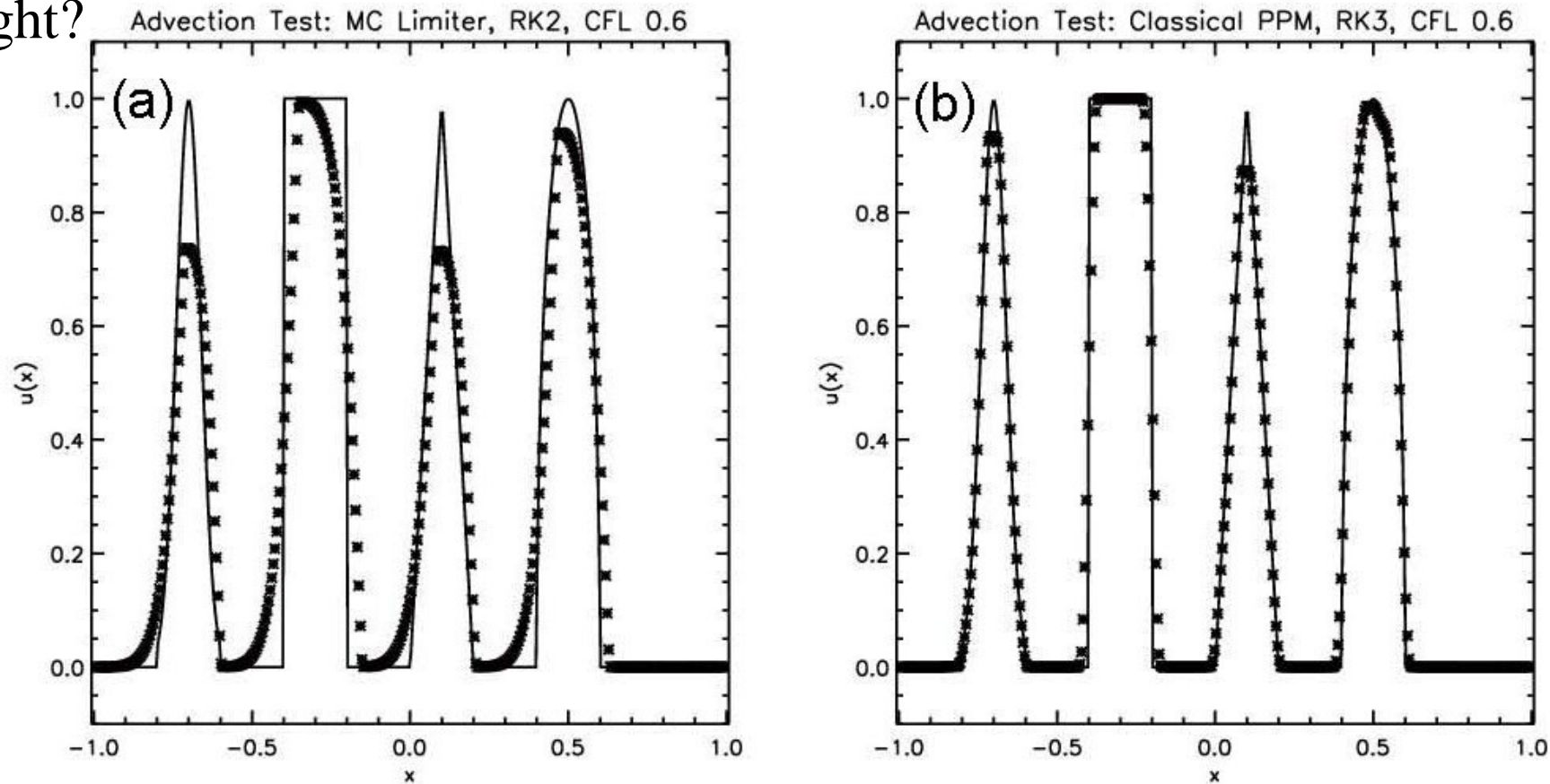


*Fig. 7.2a shows the advection test catalogued in the text when the MC limiter was used with a second order Runge-Kutta scheme. Fig. 7.2b shows the same when the classical PPM reconstruction was used with a third order Runge-Kutta scheme. The solid line shows the analytic solution, the crosses show the computed solution.*

## 7.2.2) Going Beyond Piecewise Linear: Piecewise Parabolic Reconstruction

It is only logical to think that **going beyond piecewise linear** reconstruction would yield better dividends. The **piecewise parabolic method, PPM**, is predicated on that viewpoint.

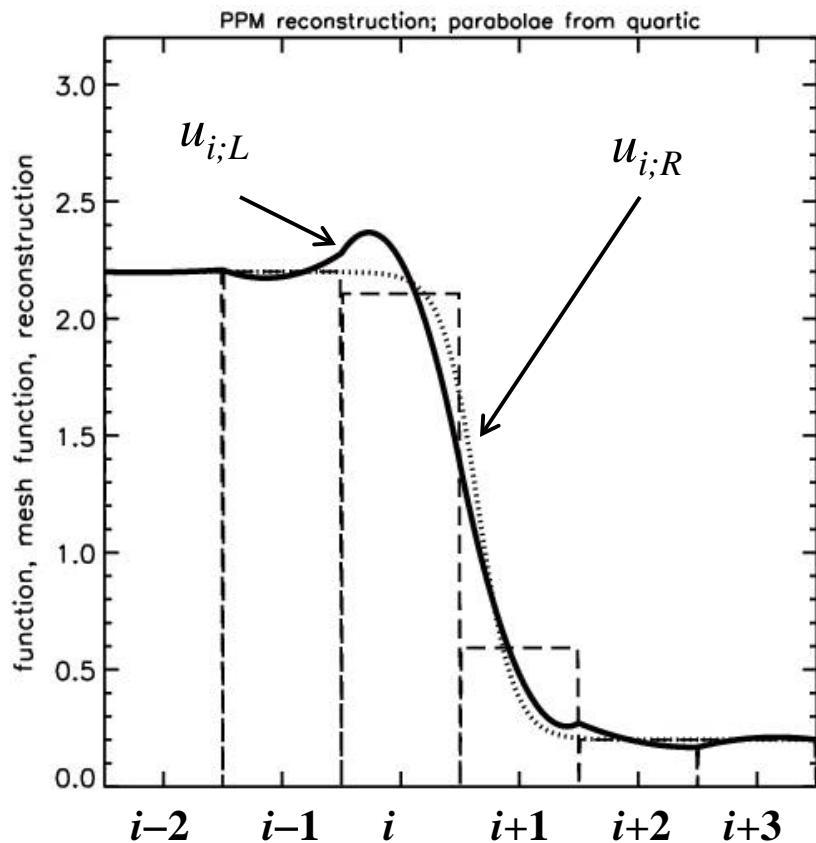
It retains a **TVD-like** flavor in that it prohibits new extrema from developing.

It is acceptable to reconstruct the variation one dimension at a time. Therefore, we focus on a one-dimensional reconstruction.

Let us assume a piecewise parabolic profile that is valid over  $[-0.5, 0.5]$ , which spans the zone “ $i$ ”:

$$u_i(x) = \bar{u}_i + \hat{u}_x x + \hat{u}_{xx} \left( x^2 - \frac{1}{12} \right)$$

Question: Why might it be beneficial to choose this form?



First, realize that  $\bar{u}$  is already specified and can't be changed.

Thus, a parabola in zone "i" would be fully specified if the left and right edge values of "u" within that zone were to be specified.

Focus on zone "i". Given  $u_{i;L}$  and  $u_{i;R}$ , we obtain:

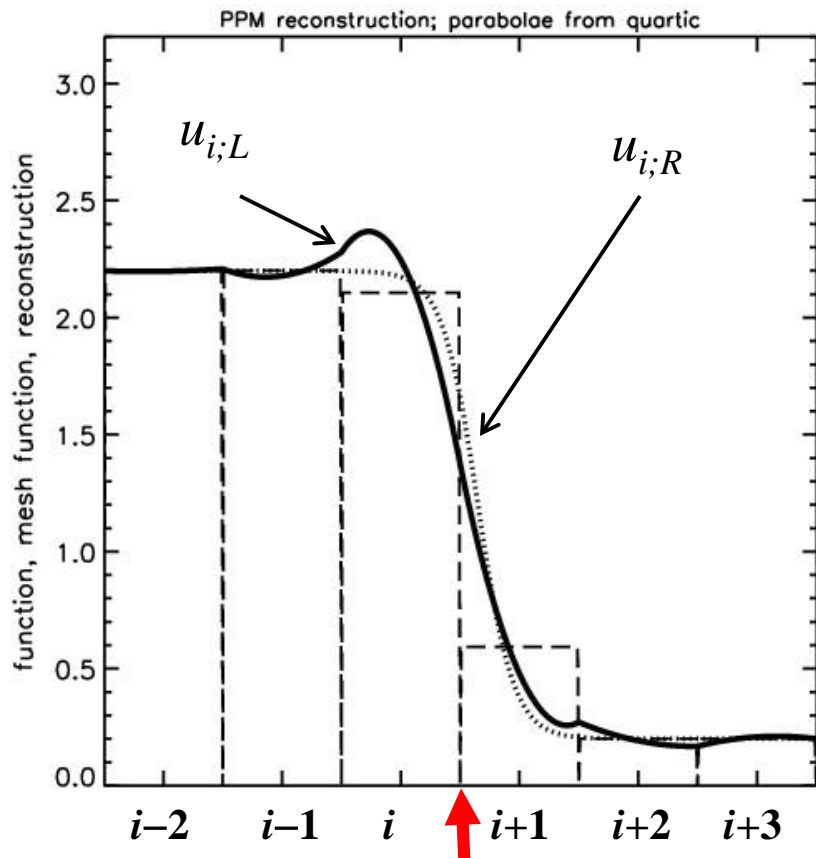
$$\hat{u}_x = u_{i;R} - u_{i;L} ; \hat{u}_{xx} = 3 u_{i;R} - 6 \bar{u}_i + 3 u_{i;L}$$

Question: So, how do we obtain  $u_{i;L}$  and  $u_{i;R}$  with third or better accuracy?

Shock-like profile shown by **dotted curve**.

Mesh function (average of shock-like profile) shown by **dashed slabs**.

**Reconstructed profile shown by solid curve**. Observe how it changes during the course of the reconstruction procedure!

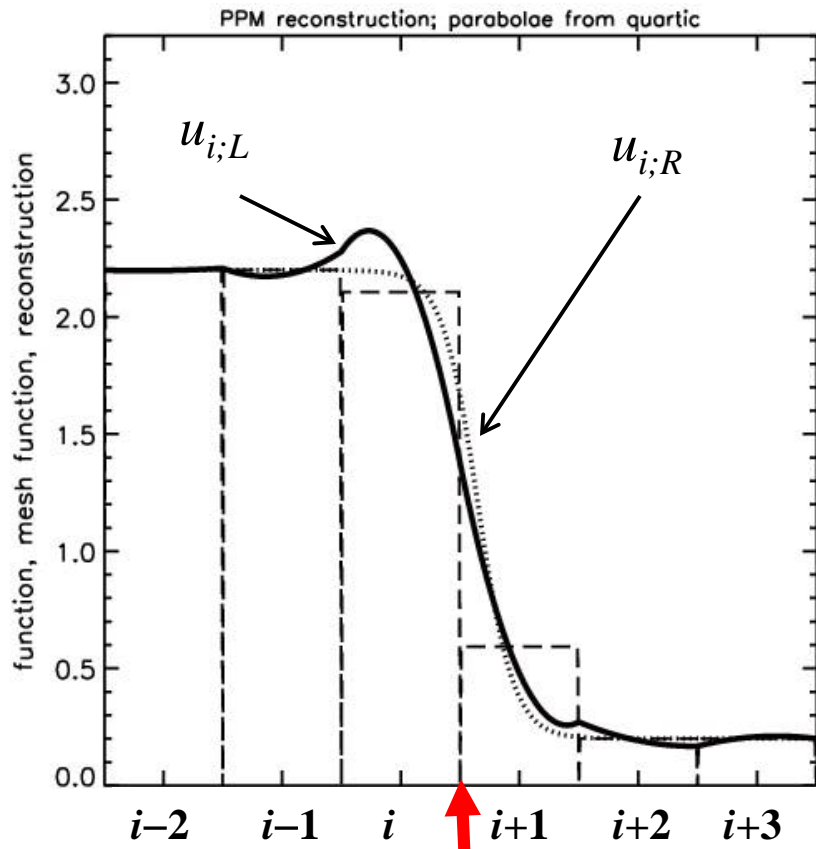


Question: So, how do we obtain  $u_{i;L}$  and  $u_{i;R}$  with third or better accuracy?

Answer: Reconstruction via primitive function:

Consider the cubic  $q(x) = q_0 + q_1x + q_2x^2 + q_3x^3$ , which is to be fitted to zones from " $i-1$ " to " $i+2$ ". This can be done by imposing the four conditions

$$\int_{-1.5}^{-0.5} q(x) dx = \bar{u}_{i-1} ; \int_{-0.5}^{0.5} q(x) dx = \bar{u}_i ; \int_{0.5}^{1.5} q(x) dx = \bar{u}_{i+1} ; \int_{1.5}^{2.5} q(x) dx = \bar{u}_{i+2}$$



Question: So, how do we obtain  $u_{i;L}$  and  $u_{i;R}$  with third or better accuracy?

$$u_{i;R} = \frac{7}{12} (\bar{u}_i + \bar{u}_{i+1}) - \frac{1}{12} (\bar{u}_{i-1} + \bar{u}_{i+2})$$

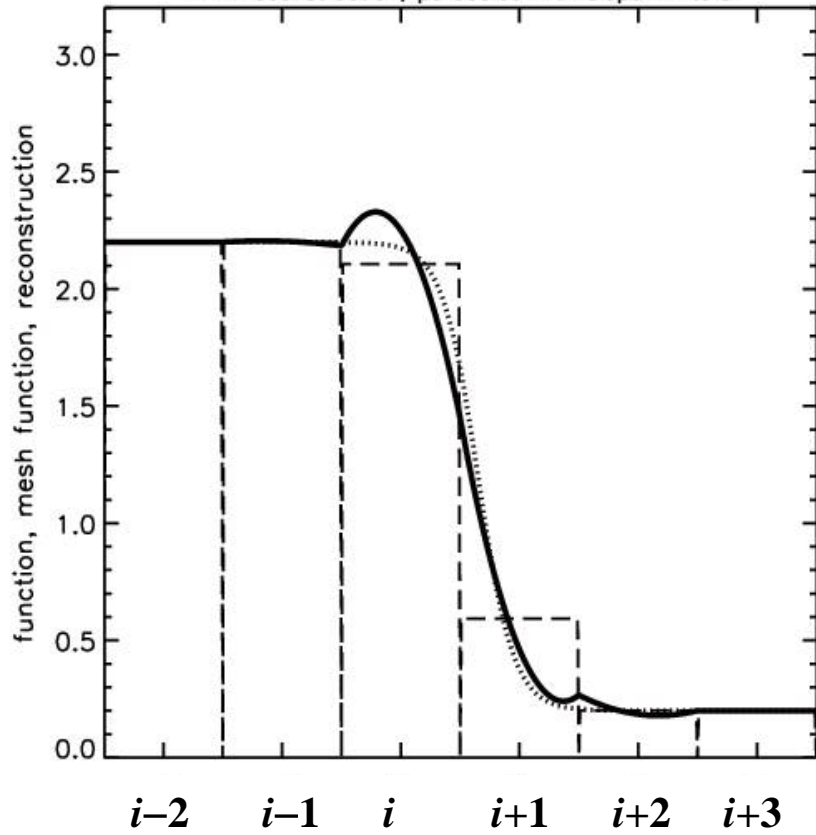
$$u_{i;R} = \bar{u}_i + \frac{1}{2} (\bar{u}_{i+1} - \bar{u}_i) - \frac{1}{6} (\Delta u_{i+1} - \Delta u_i) \text{ with } \Delta u_{i+1} = \frac{1}{2} (\bar{u}_{i+2} - \bar{u}_i) \text{ and } \Delta u_i = \frac{1}{2} (\bar{u}_{i+1} - \bar{u}_{i-1})$$

We also set  $u_{i+1;L} = u_{i;R}$ .

This parabolic profile is shown by the solid curve in the previous figure.

Question: What are the problems with the solid curve in the previous figure?

PPM reconstruction; parabola with slope limiters



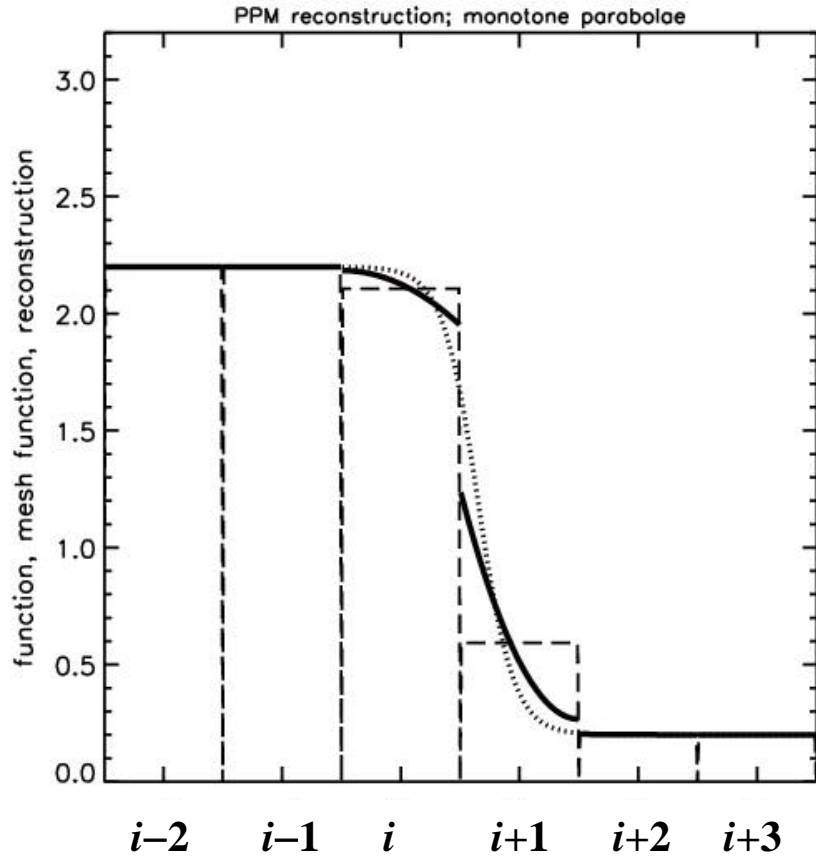
Second, consider the previous formula:

~~$$u_{i;R} = \bar{u}_i + \frac{1}{2} (\bar{u}_{i+1} - \bar{u}_i) - \frac{1}{6} (\Delta u_{i+1} - \Delta u_i) \quad \text{with} \quad \Delta u_{i+1} = \frac{1}{2} (\bar{u}_{i+2} - \bar{u}_i) \quad \text{and} \quad \Delta u_i = \frac{1}{2} (\bar{u}_{i+1} - \bar{u}_{i-1})$$~~

But now enforce a limiter. I.e., unlimited slopes above are replaced with the limited slopes below:

$$\Delta u_{i+1} = MC(\bar{u}_{i+2} - \bar{u}_{i+1}, \bar{u}_{i+1} - \bar{u}_i) \quad ; \quad \Delta u_i = MC(\bar{u}_{i+1} - \bar{u}_i, \bar{u}_i - \bar{u}_{i-1})$$

We also set  $u_{i+1;L} = u_{i;R}$ . The result is shown above. It is still unacceptable. Question: Why? 14



Third, in the spirit of not introducing new extrema, we first require that the mean value,  $\bar{u}_i$ , should lie between  $\min(u_{i,L}, u_{i,R})$  and  $\max(u_{i,L}, u_{i,R})$ . This gives us our first condition for enforcing monotonicity:

$$u_{i,L} \rightarrow \bar{u}_i \quad \text{and} \quad u_{i,R} \rightarrow \bar{u}_i \quad \text{if} \quad (u_{i,R} - \bar{u}_i)(\bar{u}_i - u_{i,L}) \leq 0$$

This condition would **flatten zone "i + 2"**.

But it leaves zones "i" and "i + 1" unchanged!

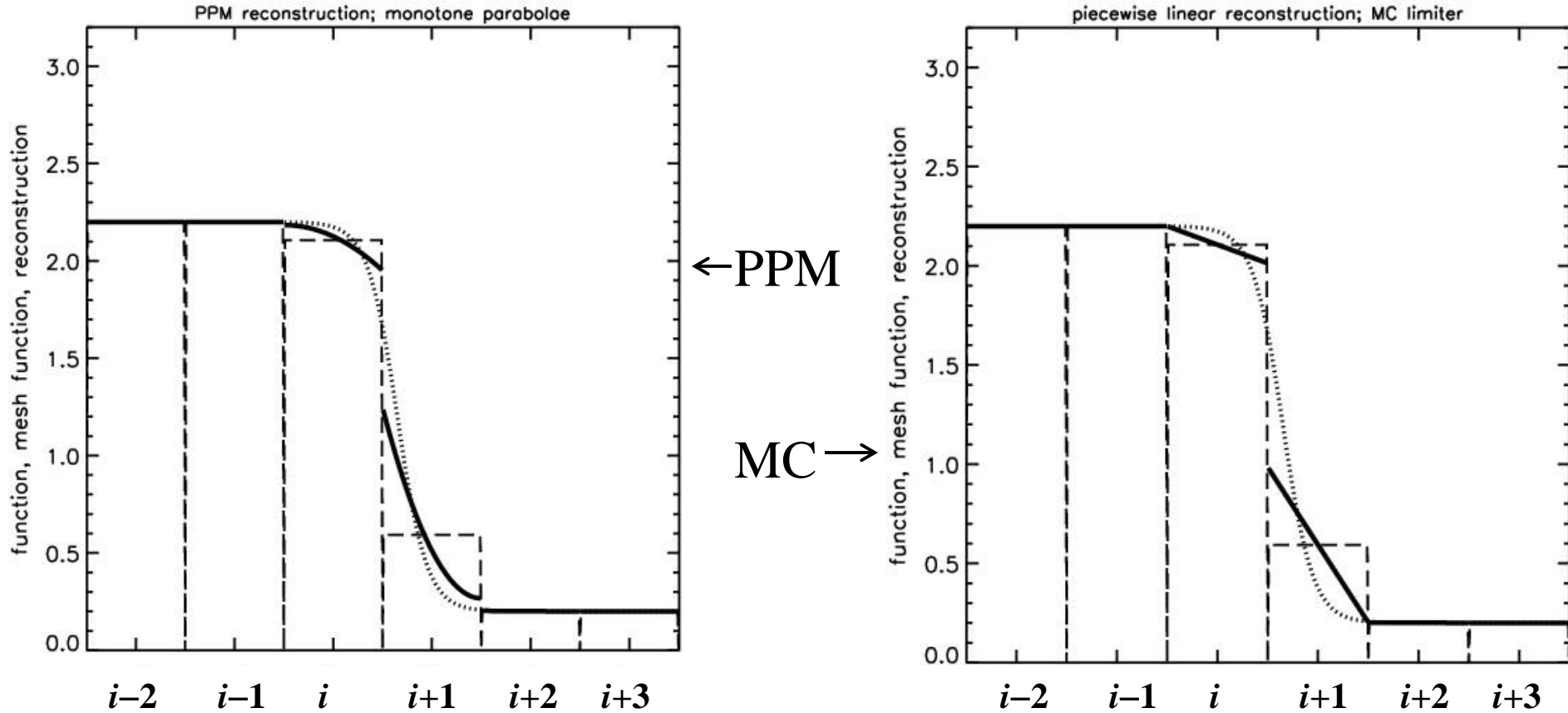
Question: How do we detect and cure those zones?

Answer: Notice that  $u_i(x) = \bar{u}_i + \hat{u}_x x + \hat{u}_{xx} \left( x^2 - \frac{1}{12} \right)$  has extrema at  $x_e = -\hat{u}_x / (2\hat{u}_{xx})$

The method **introduces a new extremum in zone "i" centered at  $x = 0$**  if:  $-0.5 < -\hat{u}_x / (2\hat{u}_{xx}) < 0.5$

Solution: **Without changing the sign of  $\hat{u}_{xx}$ , reduce the value of  $|\hat{u}_{xx}|$ .**

Question: Why will this work?



An automatic procedure for shifting the extremum out of the zone:

$$\begin{aligned}
 u_{i,L} &\rightarrow 3 \bar{u}_i - 2 u_{i,R} && \text{if } (u_{i,R} - u_{i,L}) \left( \bar{u}_i - \frac{1}{2}(u_{i,R} + u_{i,L}) \right) > \frac{(u_{i,R} - u_{i,L})^2}{6} \\
 u_{i,R} &\rightarrow 3 \bar{u}_i - 2 u_{i,L} && \text{if } - \frac{(u_{i,R} - u_{i,L})^2}{6} > (u_{i,R} - u_{i,L}) \left( \bar{u}_i - \frac{1}{2}(u_{i,R} + u_{i,L}) \right)
 \end{aligned}$$

Compare the parabolic profile above to the profile from an MC limiter.

Question: What do you see? Compare results of advection test with PPM & MC and discuss.

## 7.3) Reconstructing the Solution for Conservation Laws – Part II, Non-Oscillatory Reconstruction

The TVD and classical PPM reconstruction do **clip local extrema**, whether they are physical or not. Over thousands of timesteps, this can add up. (There are newer variants of PPM that avoid this.)

Clipping extrema  $\Leftrightarrow$  scheme is second order.

To go to higher order, we must avoid clipping *physically valid* extrema.

In Essentially Non-Oscillatory (ENO) schemes, we permit the introduction of new extrema in the reconstruction as long as the original mesh function also has such extrema.

**Weighted Essentially Non-Oscillatory (WENO)** reconstruction schemes are a modern variant.

Comes in two flavors: Finite Difference and Finite Volume

### 7.3.1) Weighted Essentially Non-Oscillatory (WENO) Reconstruction in One Dimension

Think of the **minmod limiter** as choosing from a left slope (corresponding to a **left-biased stencil**) and a right slope (corresponding to a **right-biased stencil**).

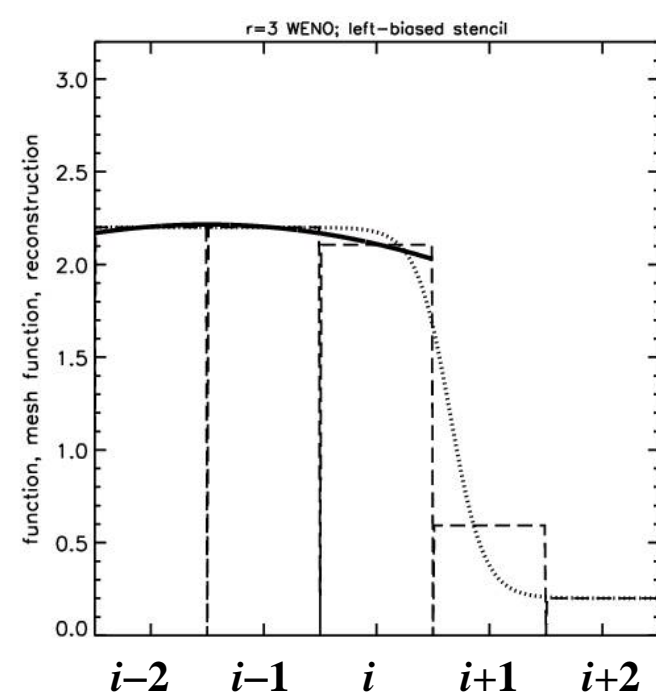
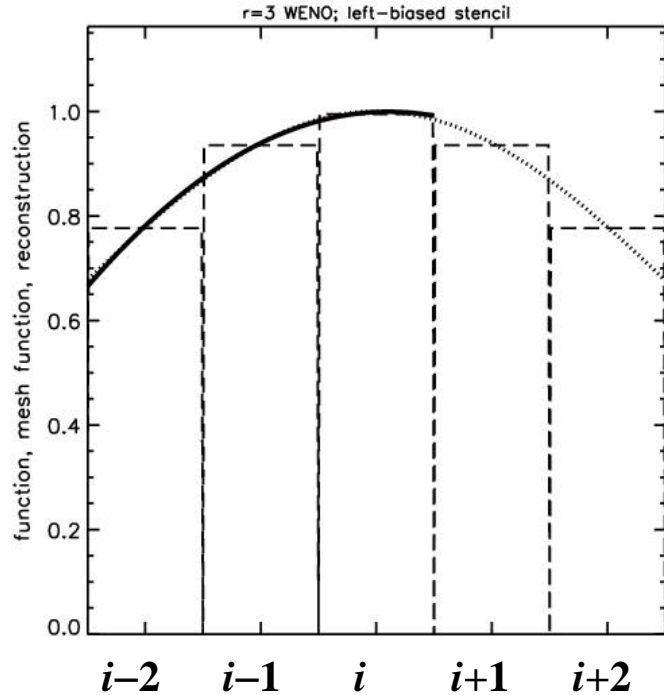
Either reconstruction is second order. Minmod chooses the stencil with the smaller slope.

The choice is made using **non-linear hybridization**.

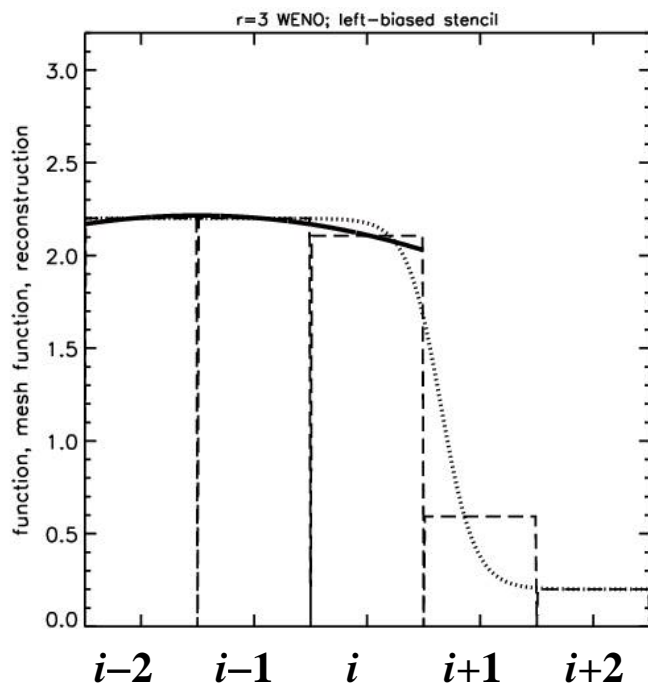
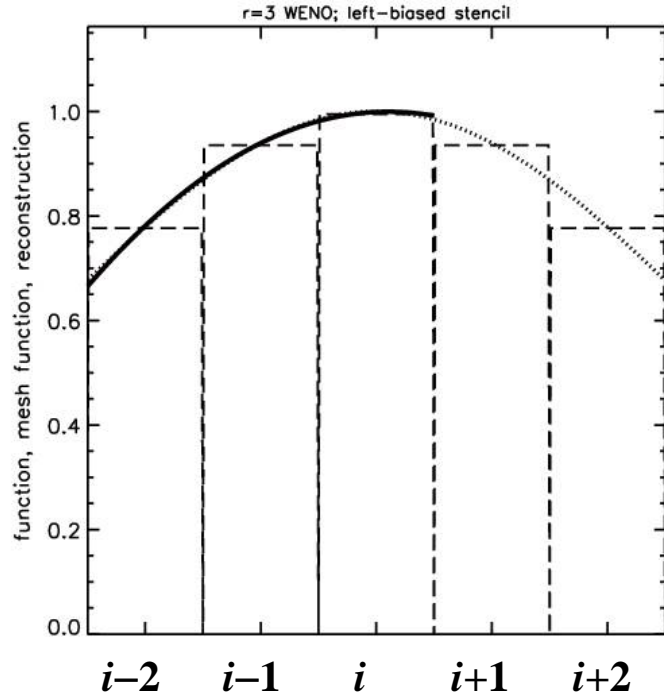
WENO takes these two ideas much further:

- 1) We do a much more detailed stencil analysis, often between two or more stencils.
- 2) The non-linear hybridization between competing stencils is also more sophisticated.

Let us see how WENO reconstructs a smooth and a discontinuous profile.



Smooth Gaussian & Shock-like profiles shown by **dotted curves**.  
 Mesh function (average of shock-like profile) shown by **dashed slabs**.  
**Reconstructed profile shown by solid curve**. Observe how it changes during the course of the reconstruction procedure!



In zone "i", we wish to reconstruct at third order

$$u_i(x) = \bar{u}_i + \hat{u}_x x + \hat{u}_{xx} \left( x^2 - \frac{1}{12} \right)$$

Because there are two moments,  $\hat{u}_x$  and  $\hat{u}_{xx}$ , we need a stencil with three zones.

First stencil is *left-biased* and covers zone "i".

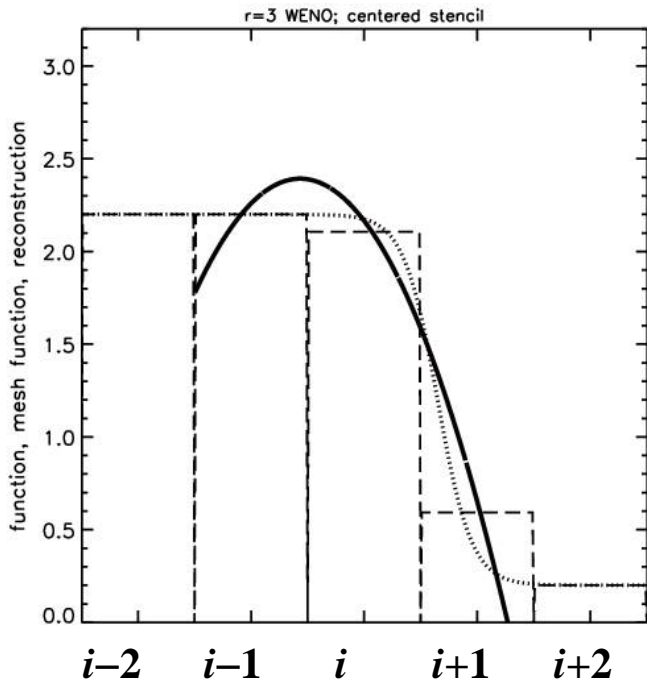
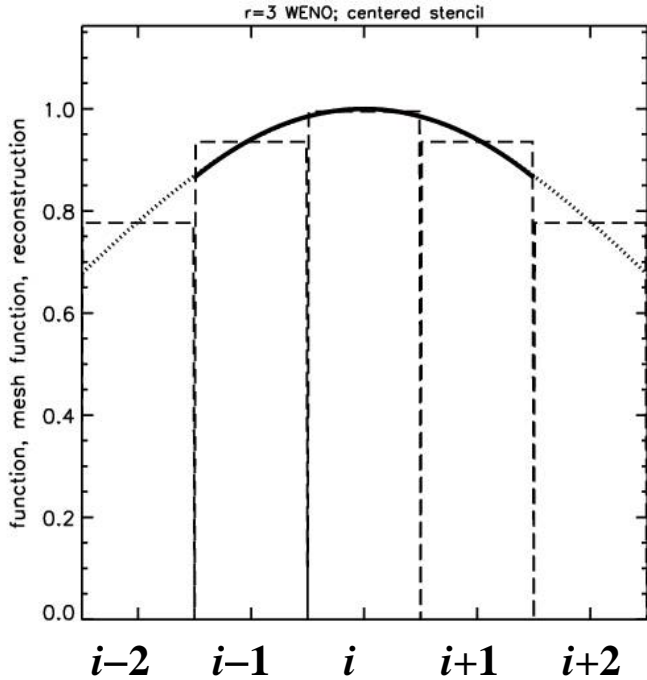
Again, **reconstruct via primitive function:**

$$\int_{-2.5}^{-1.5} u_{i,L}(x) dx = \bar{u}_{i-2} ; \int_{-1.5}^{-0.5} u_{i,L}(x) dx = \bar{u}_{i-1}$$

$$\Rightarrow \hat{u}_{L;x} = -2 \bar{u}_{i-1} + 0.5 \bar{u}_{i-2} + 1.5 \bar{u}_i ;$$

$$\hat{u}_{L;xx} = 0.5 \bar{u}_{i-2} - \bar{u}_{i-1} + 0.5 \bar{u}_i$$

Question: Can you comment on the smoothness of the two left-biased stencils? (I.e., solid curves)



Second stencil is *centrally-biased* and covers zone "i".

Again, **reconstruct via primitive function:**

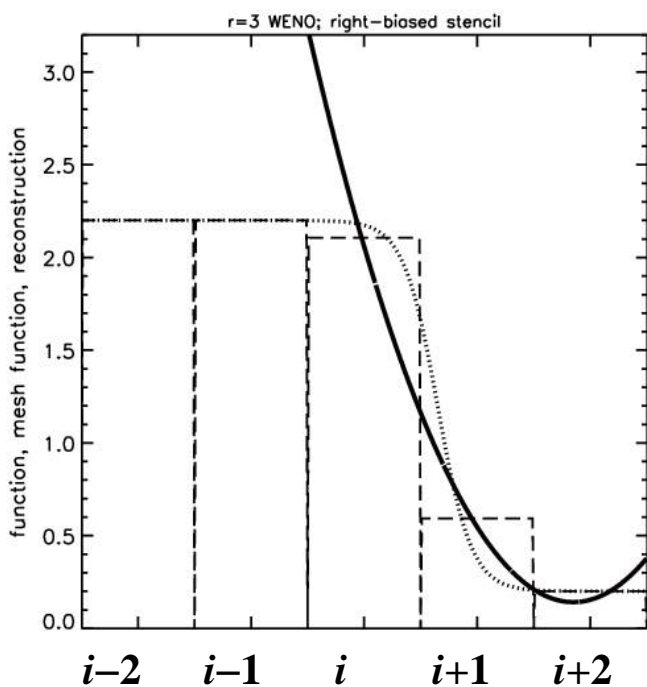
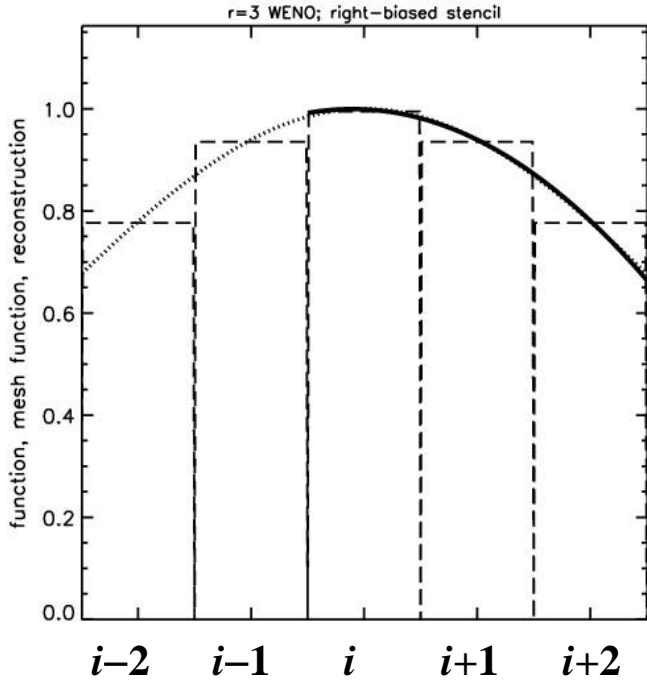
$$\int_{-1.5}^{-0.5} u_{i;C}(x) dx = \bar{u}_{i-1} ; \int_{0.5}^{1.5} u_{i;C}(x) dx = \bar{u}_{i+1}$$

$$\Rightarrow \hat{u}_{C;x} = 0.5 (\bar{u}_{i+1} + \bar{u}_{i-1}) ;$$

$$\hat{u}_{C;xx} = 0.5 \bar{u}_{i-1} - \bar{u}_i + 0.5 \bar{u}_{i+1}$$

Question: Can you comment on the smoothness of the two centrally-biased stencils? (I.e., solid curves)

Questions: Which stencil is best for stability of smooth flow? What happens when the flow is not smooth?



Third stencil is *right-biased* and covers zone "i".

Again, **reconstruct via primitive function:**

$$\int_{0.5}^{1.5} u_{i;R}(x) dx = \bar{u}_{i+1} ; \int_{1.5}^{2.5} u_{i;R}(x) dx = \bar{u}_{i+2} ;$$

$$\Rightarrow \hat{u}_{R;x} = -1.5 \bar{u}_i + 2 \bar{u}_{i+1} - 0.5 \bar{u}_{i+2} ;$$

$$\hat{u}_{R;xx} = 0.5 \bar{u}_i - \bar{u}_{i+1} + 0.5 \bar{u}_{i+2}$$

Question: Can you comment on the smoothness of the two right-biased stencils?  
(I.e., solid curves)

We need to quantify the smoothness of a stencil.

Insight: the smoothness relates to the derivatives: *larger derivatives*  $\Rightarrow$  *less smoothness*

Define smoothness indicators for each stencil:

$$IS_L = \int_{-0.5}^{0.5} \left[ \left( \frac{d u_{i;L}(x)}{dx} \right)^2 + \left( \frac{d^2 u_{i;L}(x)}{dx^2} \right)^2 \right] dx \quad \Rightarrow \quad IS_L = \hat{u}_{L;x}^2 + \frac{13}{3} \hat{u}_{L;xx}^2$$

Similarly:

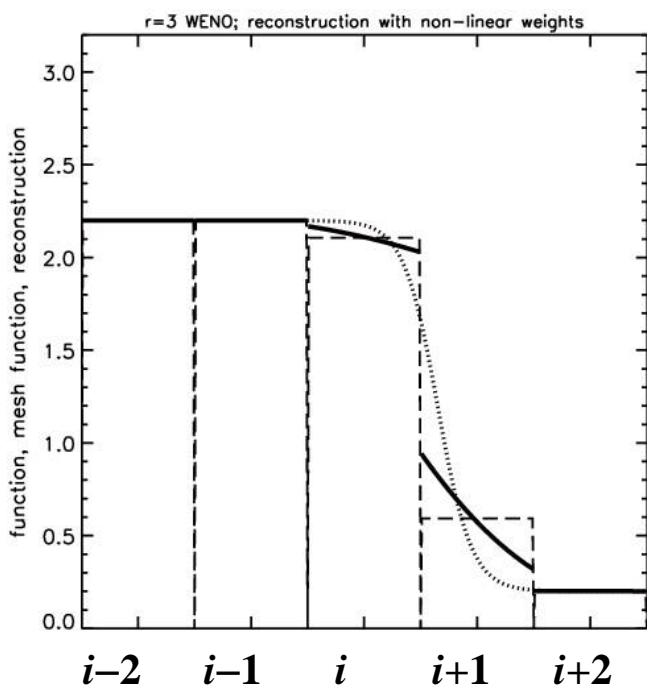
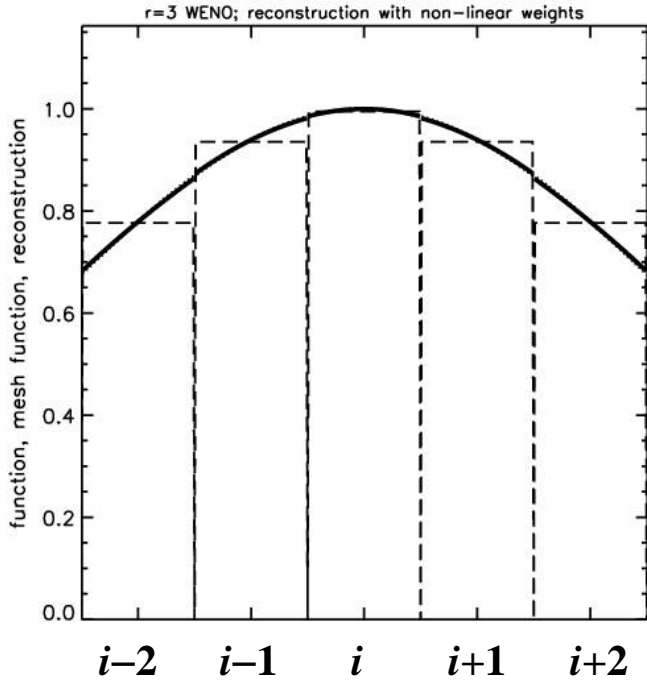
$$IS_C = \hat{u}_{C;x}^2 + \frac{13}{3} \hat{u}_{C;xx}^2 \quad \text{and} \quad IS_R = \hat{u}_{R;x}^2 + \frac{13}{3} \hat{u}_{R;xx}^2$$

Smoothness indicator is a misnomer, because the above measures actually measure how rough the solution is in each of the stencils.

Questions: What do we expect for the 3 smoothness indicators for the Gaussian?

What do we expect for the discontinuous profile?

What would happen if we keep switching back and forth too rapidly between stencils?



Solution: **Weight the stencils in inverse proportion to their smoothness indicators.**

$$w_L = \frac{\gamma_L}{(IS_L + \varepsilon)^p} ; w_C = \frac{\gamma_C}{(IS_C + \varepsilon)^p} ; w_R = \frac{\gamma_R}{(IS_R + \varepsilon)^p} ;$$

$$\bar{w}_L = \frac{w_L}{w_L + w_C + w_R} ; \bar{w}_C = \frac{w_C}{w_L + w_C + w_R} ;$$

$$\bar{w}_R = \frac{w_R}{w_L + w_C + w_R}$$

Note:  $\bar{w}_L + \bar{w}_C + \bar{w}_R = 1$

$\gamma_L$  ,  $\gamma_C$  and  $\gamma_R$  are called linear weights.

$\bar{w}_L$  ,  $\bar{w}_C$  and  $\bar{w}_R$  are called non-linear weights.

The final reconstructed profile is given by

$$\hat{u}_x = \bar{w}_L \hat{u}_{L;x} + \bar{w}_C \hat{u}_{C;x} + \bar{w}_R \hat{u}_{R;x} ;$$

$$\hat{u}_{xx} = \bar{w}_L \hat{u}_{L;xx} + \bar{w}_C \hat{u}_{C;xx} + \bar{w}_R \hat{u}_{R;xx}$$

Different strokes for different blokes:

There is a certain amount of flexibility in the choice of the linear weights, and also, indeed, in the choice of smoothness measures.

CWENO :  $\gamma_L = \gamma_R = 1$  with  $\gamma_C = 50$  and  $p=4$ .

Question: What does this do? **Central stencil is emphasized because it is more stable.**

Dispersion minimization: Requires adding further stencils.

Optimize accuracy: For right-going waves we pick  $\gamma_L = 0.1$ ,  $\gamma_C = 0.6$ ,  $\gamma_R = 0.3$

With this choice we can achieve fifth order of accuracy, but only for finite difference schemes.

This advantage of **increasing order of accuracy** does not extend to finite volume schemes.

Question: The smoothness indicators are extremely nonlinear in the solution. Why is that a good thing? What does that give you?

In general, WENO works better if the reconstruction is carried out in **characteristic variables**.

Question: Can you compare and contrast these results with those for TVD and PPM schemes?

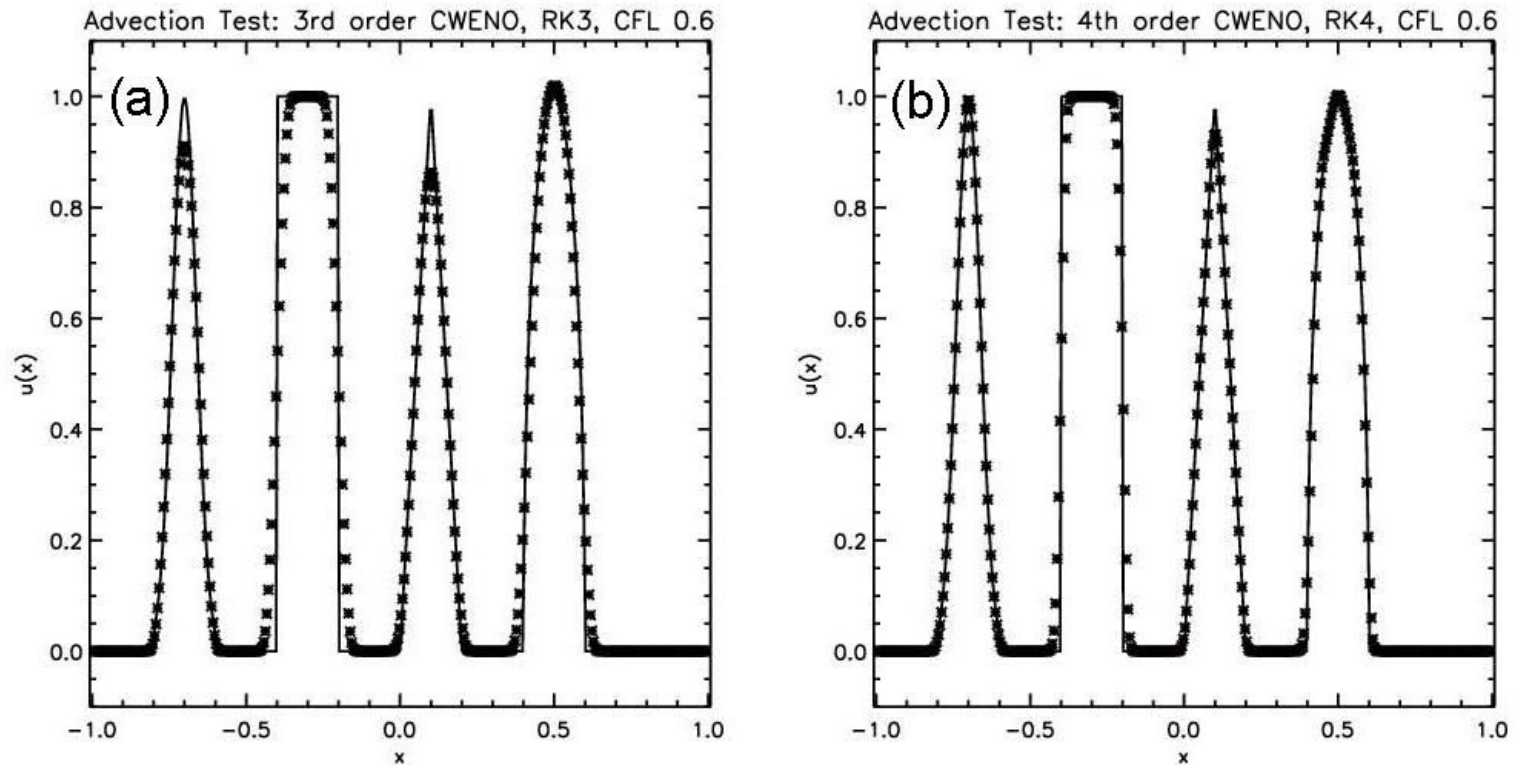


*Fig. 7.6a shows the advection test catalogued in the text when the third order CWENO reconstruction was used with a third order Runge-Kutta scheme. Fig. 7.6b shows the same when the fourth order CWENO reconstruction was used with a fourth order Runge-Kutta scheme. The solid line shows the analytic solution, the crosses show the computed solution.*

### 7.3.2) WENO Reconstruction in Multiple Dimensions

Say for example that we want third order finite volume reconstruction over a rectangular zone. We then have

$$u_{i,j}(\tilde{x}, \tilde{y}) = \bar{u}_{i,j} + \hat{u}_x \tilde{x} + \hat{u}_{xx} \left( \tilde{x}^2 - \frac{1}{12} \right) + \hat{u}_y \tilde{y} + \hat{u}_{yy} \left( \tilde{y}^2 - \frac{1}{12} \right) + \hat{u}_{xy} \tilde{x} \tilde{y}$$

Our job is to reconstruct all the moments. Can be done in one of two ways:

- 1) Choose large, multidimensional stencils, each of which yields all the moments.
- 2) Do all x-moments by looking in the x-direction; all y-moments by looking in the y-direction. Then do something special for the few cross terms that remain.

We pick strategy 2) though the book gives citations where 1) is done.

Using  $\{(i, j), (i+1, j+1)\}$  along with the consistency condition:

$$\int_{\tilde{y}=0.5}^{\tilde{y}=1.5} \int_{\tilde{x}=0.5}^{\tilde{x}=1.5} u_{i,j}(\tilde{x}, \tilde{y}) d\tilde{x} d\tilde{y} = \bar{u}_{i+1,j+1}$$

gives

$$\hat{u}_{xy} = \bar{u}_{i+1,j+1} - \bar{u}_{i,j} - \hat{u}_x - \hat{u}_y - \hat{u}_{xx} - \hat{u}_{yy}$$

Three other stencils are possible. Question: Can you list the other three stencils?

The smoothness indicators are given by :  $IS = 4 \hat{u}_{xx}^2 + 4 \hat{u}_{yy}^2 + \hat{u}_{xy}^2$

The resulting non-linear hybridization is obvious.

## 7.4) Evolving Conservation Laws Accurately in Time – Part I, Runge-Kutta Methods

Spatial reconstruction at second and third order has been thoroughly discussed. Even higher orders of spatial reconstruction are possible.

To get a **balanced scheme**, the **temporal accuracy must match the spatial accuracy**.

Easiest way to do that is given by Runge-Kutta methods.

The time evolution is conceptualized as the solution of an ordinary differential equation. Recall the terminology, “**method of lines**”, “**semi-discrete approximation**” from Lecture 2.

Each stage in a Runge-Kutta method is simple and multiple **internal stages** make up the RK method to give us the overall time accuracy.

Only some classes of RK methods preserve the TVD property – **SSP-RK**.

## 7.4.1) Runge-Kutta Time Stepping

Conceptualize this as an evolution in time:  $\frac{\partial \mathbf{U}}{\partial t} = L(\mathbf{U}) \equiv -\mathbf{F}(\mathbf{U})_x - \mathbf{G}(\mathbf{U})_y$

Improved Euler approximation is **Strong Stability Preserving (SSP)** and **second order**:

Question: What does SSP do for us?

$$\mathbf{U}^{(1)} = \mathbf{U}^n + \Delta t L(\mathbf{U}^n)$$

$$\mathbf{U}^{n+1} = \frac{1}{2} \mathbf{U}^n + \frac{1}{2} \mathbf{U}^{(1)} + \frac{1}{2} \Delta t L(\mathbf{U}^{(1)})$$

Can we extend this to third order RK-SSP? Yes!

$$\mathbf{U}^{(1)} = \mathbf{U}^n + \Delta t L(\mathbf{U}^n)$$

$$\mathbf{U}^{(2)} = \frac{3}{4} \mathbf{U}^n + \frac{1}{4} \mathbf{U}^{(1)} + \frac{1}{4} \Delta t L(\mathbf{U}^{(1)})$$

$$\mathbf{U}^{n+1} = \frac{1}{3} \mathbf{U}^n + \frac{2}{3} \mathbf{U}^{(2)} + \frac{2}{3} \Delta t L(\mathbf{U}^{(2)})$$

Above two schemes support a max CFL of unity in 1D; Question: What about multi-d?

Question: To what orders can we continue this?

Answer: From **4th order** onwards, **RK-SSP** schemes become quite complicated

-- **Butcher barriers!**

Fourth order RK-SSP scheme

$$U^{(1)} = U^n + 0.39175222700392 \Delta t L(U^n)$$

$$U^{(2)} = 0.44437049406734 U^n + 0.55562950593266 U^{(1)} + 0.36841059262959 \Delta t L(U^{(1)})$$

$$U^{(3)} = 0.62010185138540 U^n + 0.37989814861460 U^{(2)} + 0.25189177424738 \Delta t L(U^{(2)})$$

$$U^{(4)} = 0.17807995410773 U^n + 0.82192004589227 U^{(3)} + 0.54497475021237 \Delta t L(U^{(3)})$$

$$U^{n+1} = 0.00683325884039 U^n + 0.51723167208978 U^{(2)}$$

$$+ 0.12759831133288 U^{(3)} + 0.34833675773694 U^{(4)}$$

$$+ 0.08460416338212 \Delta t L(U^{(3)}) + 0.22600748319395 \Delta t L(U^{(4)})$$

## 7.4.2) Second Order Accurate Runge-Kutta Scheme

We can now discretize the spatial parts of the governing equation as

$$\frac{\partial \bar{U}_{i,j}}{\partial t} = L(\bar{U})_{i,j} = -\frac{1}{\Delta x} \left( \bar{F}_{i+1/2,j} - \bar{F}_{i-1/2,j} \right) - \frac{1}{\Delta y} \left( \bar{G}_{i,j+1/2} - \bar{G}_{i,j-1/2} \right)$$

with

$$\bar{F}_{i+1/2,j} \equiv \int_{\tilde{y}=-1/2}^{\tilde{y}=1/2} F(\tilde{x}=1/2, \tilde{y}) d\tilde{y} \quad ; \quad \bar{G}_{i,j+1/2} \equiv \int_{\tilde{x}=-1/2}^{\tilde{x}=1/2} G(\tilde{x}, \tilde{y}=1/2) d\tilde{x}$$

The **integration** of the fluxes along the faces reminds us that we are dealing with a **finite volume formulation**. The integration of the fluxes should be done with **sufficiently high order of spatial accuracy** in order to realize the full accuracy of the method.

**At second order things are simple.** We can replace the spatially averaged fluxes with the fluxes from the Riemann problem that have been evaluated at the centers of the zone faces.

In each zone  $(i, j)$ , we assume we have  $\bar{U}_{i,j}$  and undivided differences  $\Delta_x \bar{U}_{i,j}$  and  $\Delta_y \bar{U}_{i,j}$ , to get:

$$U_{L;i+1/2,j} = \bar{U}_{i,j} + \frac{1}{2} \Delta_x \bar{U}_{i,j} \quad ; \quad U_{R;i+1/2,j} = \bar{U}_{i+1,j} - \frac{1}{2} \Delta_x \bar{U}_{i+1,j}$$

$$U_{B;i,j+1/2} = \bar{U}_{i,j} + \frac{1}{2} \Delta_y \bar{U}_{i,j} \quad ; \quad U_{T;i,j+1/2} = \bar{U}_{i,j+1} - \frac{1}{2} \Delta_y \bar{U}_{i,j+1}$$

$$\bar{F}_{i+1/2,j} = F_{RS} \left( U_{L;i+1/2,j}, U_{R;i+1/2,j} \right) \quad ; \quad \bar{G}_{i,j+1/2} = G_{RS} \left( U_{B;i,j+1/2}, U_{T;i,j+1/2} \right)$$

The neighboring zones have to interact using a Riemann solver so that we get the flux at the zone boundaries!

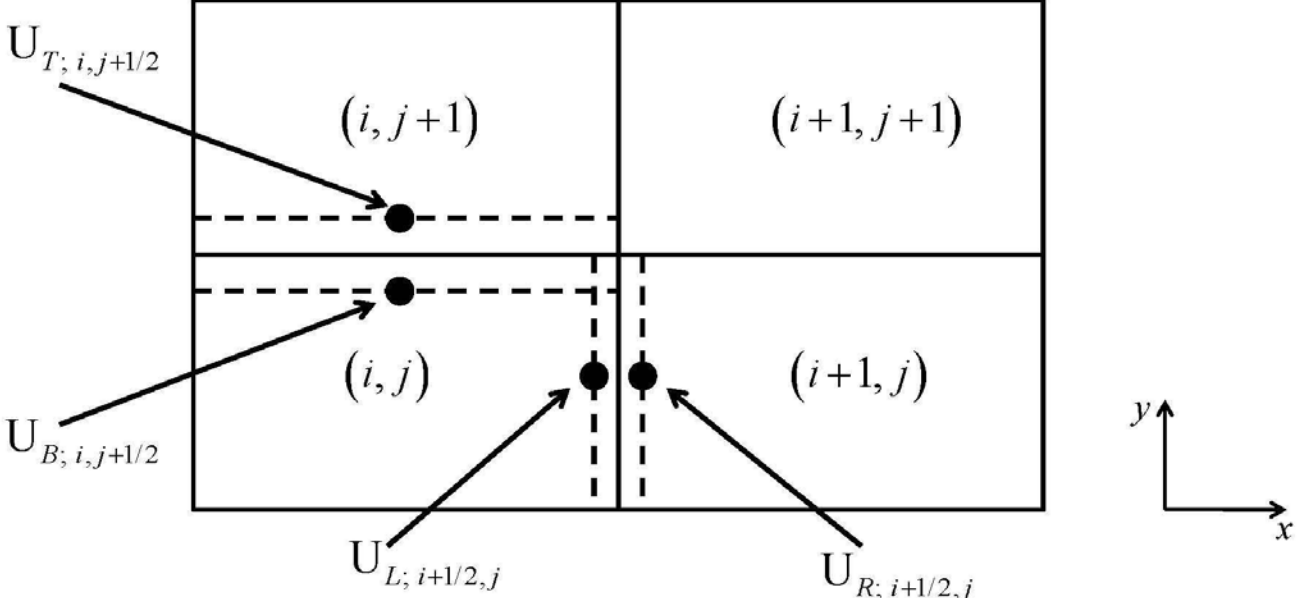


Fig. 7.7 shows the construction for obtaining spatially second order accurate fluxes for the second order Runge-Kutta scheme. The quadrature points are shown with dots. The surfaces to the immediate left and immediate right of the zone boundaries are shown with dashes.

### 7.4.3) Runge-Kutta Schemes at Higher Orders; Using Third Order as an Example

We still discretize the spatial parts of the governing equation as

$$\frac{\partial \bar{U}_{i,j}}{\partial t} = L(\bar{U})_{i,j} = -\frac{1}{\Delta x} \left( \bar{F}_{i+1/2,j} - \bar{F}_{i-1/2,j} \right) - \frac{1}{\Delta y} \left( \bar{G}_{i,j+1/2} - \bar{G}_{i,j-1/2} \right)$$

with

$$\bar{F}_{i+1/2,j} \equiv \int_{\tilde{y}=-1/2}^{\tilde{y}=1/2} F(\tilde{x} = 1/2, \tilde{y}) d\tilde{y} \quad ; \quad \bar{G}_{i,j+1/2} \equiv \int_{\tilde{x}=-1/2}^{\tilde{x}=1/2} G(\tilde{x}, \tilde{y} = 1/2) d\tilde{x}$$

Problem: **At higher order**, evaluating the above integrals becomes difficult.

Questions: What does the **Simpson rule** tell us about numerical quadrature?

How many evaluations of the numerical flux would it require?

One option would be to use **multiple Riemann solver evaluations** at multiple **Gaussian points** along each boundary. This can become very **expensive**.

Because Riemann problem evaluation is expensive, we want to make as few evaluations of the Riemann problem as possible -- A **quadrature - free approach**.<sup>34</sup>

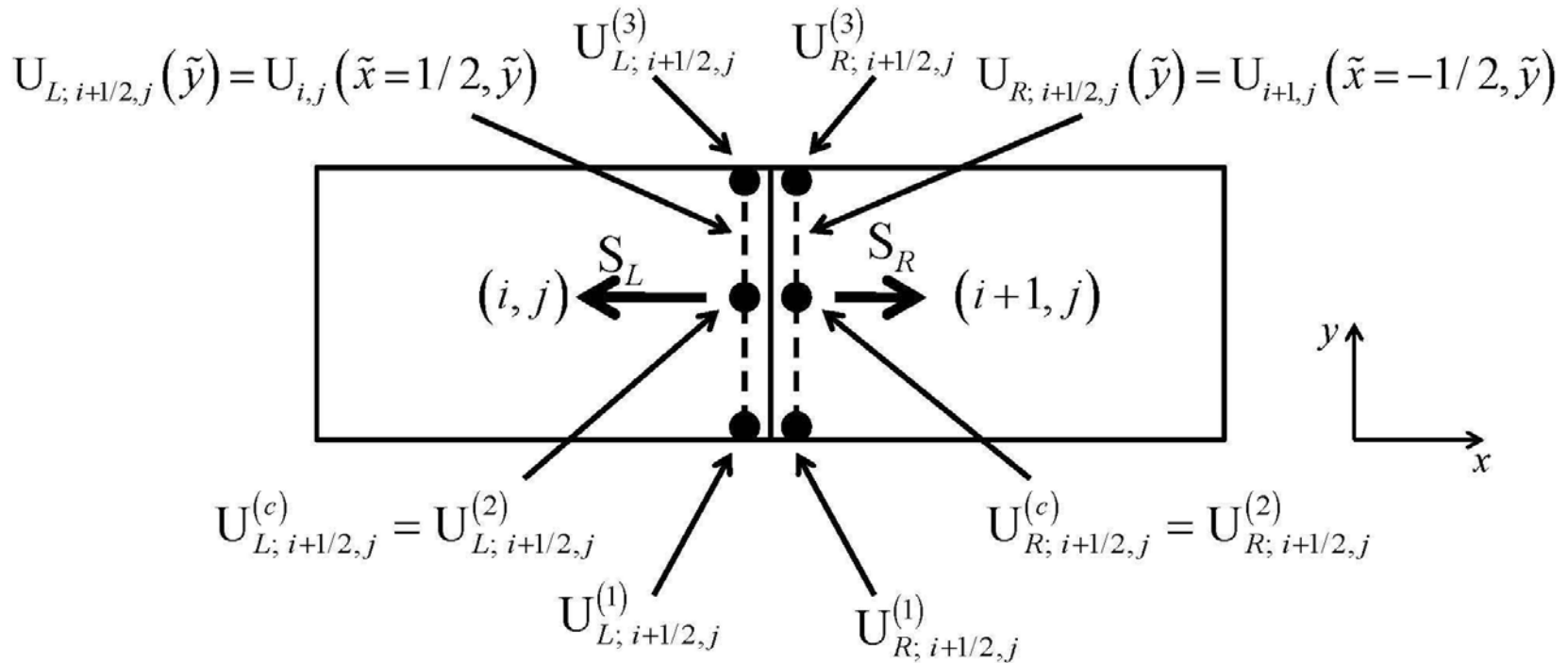
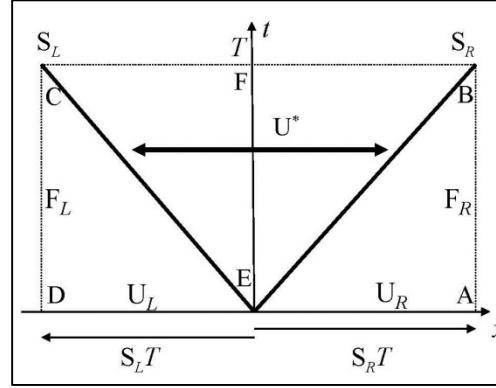


Fig. 7.8 shows the construction for obtaining spatially third order accurate fluxes for the third order Runge-Kutta scheme. The wave model, along with the variables used for obtaining it, are shown. The quadrature points are shown with dots. The surfaces to the immediate left and immediate right of the zone boundary at  $(i+1/2, j)$  are shown with dashes.

Start with a reconstructed profile in each zone  $(i, j)$ :

$$U_{i,j}(\tilde{x}, \tilde{y}) = \bar{U}_{i,j} + \hat{U}_{i,j;x} \tilde{x} + \hat{U}_{i,j;y} \tilde{y} + \hat{U}_{i,j;xx} \left( \tilde{x}^2 - \frac{1}{12} \right) + \hat{U}_{i,j;yy} \left( \tilde{y}^2 - \frac{1}{12} \right) + \hat{U}_{i,j;xy} \tilde{x} \tilde{y}$$

Let us take the HLL Riemann solver as an example.

$U_{i,j}(\tilde{x}, \tilde{y})$  is used to obtain the left state :  $U_{L; i+1/2,j}^{(c)} = U_{i,j}(\tilde{x} = 1/2, \tilde{y} = 0)$

$U_{i+1,j}(\tilde{x}, \tilde{y})$  is used to obtain the right state :  $U_{R; i+1/2,j}^{(c)} = U_{i+1,j}(\tilde{x} = -1/2, \tilde{y} = 0)$

These can be used to obtain  $S_L$  and  $S_R$ , the extremal wave speeds for the HLL RS.

If these wave speeds are frozen, we obtain the HLL flux as:

$$\begin{aligned} F_{i+1/2,j}(\tilde{y}) = & \left[ \frac{S_R}{S_R - S_L} \right] F_{L; i+1/2,j}(\tilde{y}) - \left[ \frac{S_L}{S_R - S_L} \right] F_{R; i+1/2,j}(\tilde{y}) \\ & + \left[ \frac{S_R S_L}{S_R - S_L} \right] (U_{R; i+1/2,j}(\tilde{y}) - U_{L; i+1/2,j}(\tilde{y})) \end{aligned}$$

Question: What does freezing the wave speeds,  $S_L$  and  $S_R$ , give us?

The reconstruction within each zone allows us to write:

$$U_{L; i+1/2, j}(\tilde{y}) = U_{i, j}(\tilde{x} = 1/2, \tilde{y}) \quad ; \quad U_{R; i+1/2, j}(\tilde{y}) = U_{i+1, j}(\tilde{x} = -1/2, \tilde{y})$$

The above expressions are available analytically and can be integrated once and for all:

$$\begin{aligned} & \int_{\tilde{y}=-1/2}^{\tilde{y}=1/2} \left( U_{R; i+1/2, j}(\tilde{y}) - U_{L; i+1/2, j}(\tilde{y}) \right) d\tilde{y} \\ &= \left( \bar{U}_{i+1, j} - \frac{1}{2} \hat{U}_{i+1, j; x} + \frac{1}{6} \hat{U}_{i+1, j; xx} \right) - \left( \bar{U}_{i, j} + \frac{1}{2} \hat{U}_{i, j; x} + \frac{1}{6} \hat{U}_{i, j; xx} \right) \end{aligned}$$

Fluxes treated similarly:

$$U_{L; i+1/2, j}^{(1)} = U_{i, j}(\tilde{x} = 1/2, \tilde{y} = -1/2) \quad ; \quad U_{L; i+1/2, j}^{(2)} = U_{i, j}(\tilde{x} = 1/2, \tilde{y} = 0) \quad ;$$

$$U_{L; i+1/2, j}^{(3)} = U_{i, j}(\tilde{x} = 1/2, \tilde{y} = 1/2)$$

$$\int_{\tilde{y}=-1/2}^{\tilde{y}=1/2} F_{L; i+1/2, j}(\tilde{y}) d\tilde{y} = \frac{1}{6} F(U_{L; i+1/2, j}^{(1)}) + \frac{2}{3} F(U_{L; i+1/2, j}^{(2)}) + \frac{1}{6} F(U_{L; i+1/2, j}^{(3)})$$

## 7.5) Evolving Conservation Laws Accurately in Time – Part II, Predictor-Corrector Schemes

### 7.5.1) Second Order Accurate Predictor-Corrector Schemes

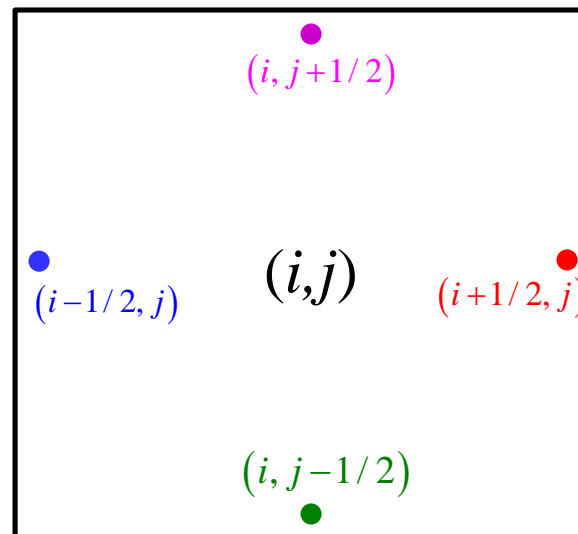
Say we have used the reconstruction in zone  $(i, j)$  at time  $t^n$  to obtain:

$$U_{i,j}^n(\tilde{x}, \tilde{y}) = \bar{U}_{i,j}^n + \Delta_x \bar{U}_{i,j} \tilde{x} + \Delta_y \bar{U}_{i,j} \tilde{y}$$

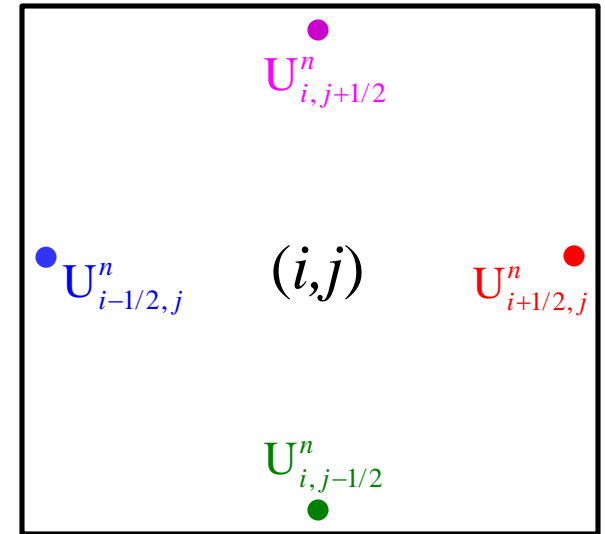
We refer to  $\Delta_x \bar{U}_{i,j}$  and  $\Delta_y \bar{U}_{i,j}$  as the modes.

Consider *nodal points* :  $(i+1/2, j)$ ,  $(i-1/2, j)$ ,  $(i, j+1/2)$  and  $(i, j-1/2)$ .

We evaluate nodal values from immediately inside the zone  $(i, j)$  being considered.



The Predictor Step now gives us an “**evolution-in-the-small**” for the PDE as follows:-



Consider *nodal points* :  $(i+1/2, j)$ ,  $(i-1/2, j)$ ,  $(i, j+1/2)$  and  $(i, j-1/2)$ .

We now have *nodal values*:  $U_{i+1/2,j}^n = \bar{U}_{i,j}^n + \frac{1}{2} \Delta_x \bar{U}_{i,j}$ ;  $U_{i-1/2,j}^n = \bar{U}_{i,j}^n - \frac{1}{2} \Delta_x \bar{U}_{i,j}$  ;  
 $U_{i,j+1/2}^n = \bar{U}_{i,j}^n + \frac{1}{2} \Delta_y \bar{U}_{i,j}$ ;  $U_{i,j-1/2}^n = \bar{U}_{i,j}^n - \frac{1}{2} \Delta_y \bar{U}_{i,j}$

Predictor Step then gives us the time rate of update within each zone  $(i, j)$  as:

$$\left( \frac{\partial U}{\partial t} \right)_{i,j}^n = -\frac{1}{\Delta x} \left( F(U_{i+1/2,j}^n) - F(U_{i-1/2,j}^n) \right) - \frac{1}{\Delta y} \left( G(U_{i,j+1/2}^n) - G(U_{i,j-1/2}^n) \right)$$

Corrector Step then assembles the space- and time-centered values on either side of each zone boundary:

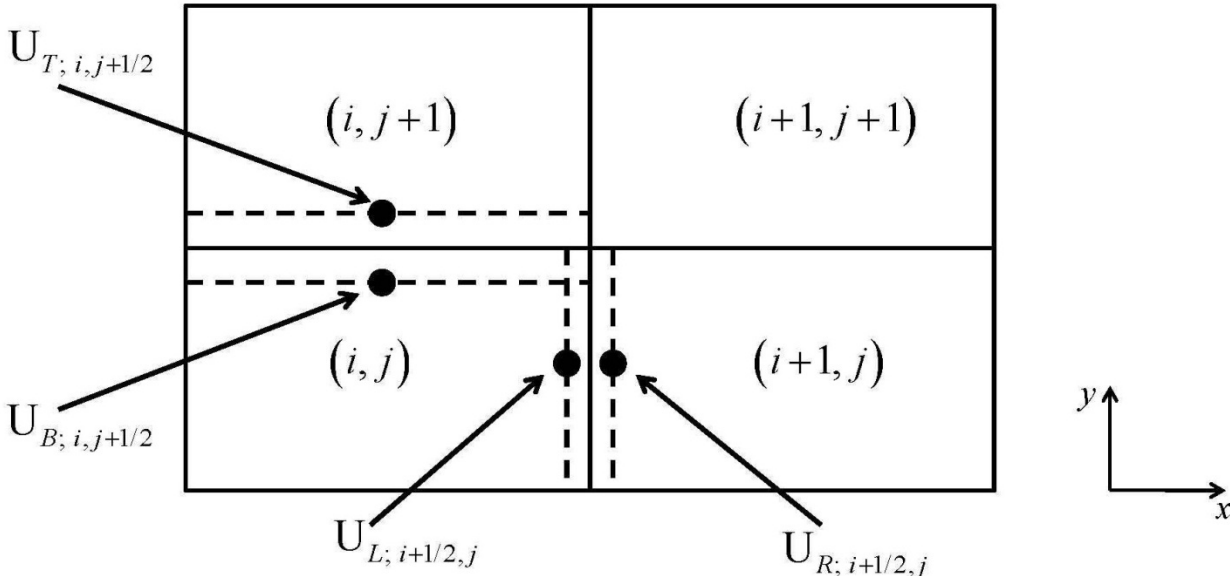
$$U_{L;i+1/2,j}^{n+1/2} \equiv \bar{U}_{i,j}^n + \frac{1}{2} \Delta_x \bar{U}_{i,j}^n + \frac{1}{2} \Delta t \left( \frac{\partial U}{\partial t} \right)_{i,j}^n ; U_{R;i+1/2,j}^{n+1/2} \equiv \bar{U}_{i+1,j}^n - \frac{1}{2} \Delta_x \bar{U}_{i+1,j}^n + \frac{1}{2} \Delta t \left( \frac{\partial U}{\partial t} \right)_{i+1,j}^n$$

$$U_{B;i,j+1/2}^{n+1/2} \equiv \bar{U}_{i,j}^n + \frac{1}{2} \Delta_y \bar{U}_{i,j}^n + \frac{1}{2} \Delta t \left( \frac{\partial U}{\partial t} \right)_{i,j}^n ; U_{T;i,j+1/2}^{n+1/2} \equiv \bar{U}_{i,j+1}^n - \frac{1}{2} \Delta_y \bar{U}_{i,j+1}^n + \frac{1}{2} \Delta t \left( \frac{\partial U}{\partial t} \right)_{i,j+1}^n$$

Final update:

$$\bar{U}_{i,j}^{n+1} = \bar{U}_{i,j}^n - \frac{\Delta t}{\Delta x} \left( F_{RS} \left( U_{L;i+1/2,j}^{n+1/2}, U_{R;i+1/2,j}^{n+1/2} \right) - F_{RS} \left( U_{L;i-1/2,j}^{n+1/2}, U_{R;i-1/2,j}^{n+1/2} \right) \right) - \frac{\Delta t}{\Delta y} \left( G_{RS} \left( U_{B;i,j+1/2}^{n+1/2}, U_{T;i,j+1/2}^{n+1/2} \right) - G_{RS} \left( U_{B;i,j-1/2}^{n+1/2}, U_{T;i,j-1/2}^{n+1/2} \right) \right)$$

The Corrector Step is the step where the neighboring zones interact with each other through the **Riemann solver**.



## 7.5.2) ADER Time Stepping for Second, and Higher Order Time Accuracy

**ADER** == **A**rbitrary **DER**ivatives in space and time.

It is a method for starting with a high order spatial reconstruction and rapidly doing the time update with higher order of accuracy.

I.e., the **Predictor-Corrector** methods at second order go on to become full-fledged **ADER methods** at all orders in space and time.

The important part is the ADER-Predictor step. It starts with the spatially reconstructed modes with any order of **spatial accuracy** within a zone. It gives us the temporal “**evolution-in-the-small**” of the PDE up to the **same order of space-time accuracy**. Here, “evolution-in-the-small” means locally within the zone of interest.

ADER-CG studied here. “CG” stands for Continuous Galerkin.

Question: What does a stiff source term do?

**1D ADER Predictor In Brief** ; Toro & Titarev (2002), Titarev & Toro (2002), Gassner et al (2007), Dumbser, Enaux & Toro (2008), Dumbser *et al.* (2008) Toro & Castro (2008), Gassner et al (2011), Balsara *et al.* (2009, 2013)

$$\text{Governing Equation : } \partial_t u + \partial_x f(u) = 0$$

Mathematical Statement of our goal:-

Within a 1D zone start with **spatial reconstruction**, i.e. **spatial modes**:-

$$u(x, t=0) = \hat{w}_0 + \hat{w}_x x + \hat{w}_{xx} \left( x^2 - \frac{1}{12} \right)$$

Use **governing equation** to obtain **space-time reconstruction**, i.e. **space-time modes**:-

$$u(x, t) = \hat{w}_0 + \hat{w}_x x + \hat{w}_{xx} \left( x^2 - \frac{1}{12} \right) + \hat{u}_t t + \hat{u}_{tt} t^2 + \hat{u}_{xt} x t \leftarrow \text{Dynamics!!!}$$

The process is **iterative**, but the iterations converge very **fast**!

$$\text{Governing Equation : } \partial_t u + \partial_x f(u) = 0$$

STEP I) Start with the reconstructed initial polynomial **within each zone** expressed in a **higher order modal basis** set (i.e. orthogonal Hermite polynomials) (1d here for simplicity; *modes shown with caret*):-

$$u(x, t=0) = \hat{w}_0 + \hat{w}_x x + \hat{w}_{xx} \left( x^2 - \frac{1}{12} \right)$$

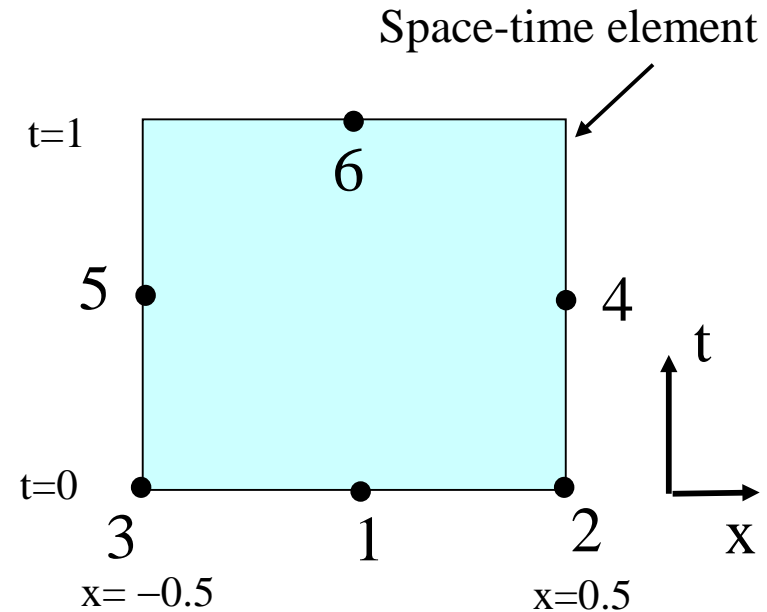
We can use the above to obtain the spatial representation of the fluxes at  $t=0$ ;

i.e. **evaluate only once**:

$$f(x, t=0) = \hat{f}_0 + \hat{f}_x x + \hat{f}_{xx} \left( x^2 - \frac{1}{12} \right)$$

How? Answer:

- Evaluate  $u_1 = u(x=0, t=0)$ ,  $u_2 = u(x=.5, t=0)$ ,  $u_3 = u(x=-.5, t=0)$ .
- Find  $f_1 = f(u_1)$ ,  $f_2 = f(u_2)$ ,  $f_3 = f(u_3)$ .
- Obtain modal representation of flux. **3<sup>rd</sup> order in 1D is first non-trivial case.**



$$\text{Governing Equation : } \partial_t u + \partial_x f(u) = 0$$

### STEP I, cont'd)

We wish to obtain the space-time representation of the conserved vars. within a zone:-

$$u(x, t) = \hat{w}_0 + \hat{w}_x x + \hat{w}_{xx} \left( x^2 - \frac{1}{12} \right) + \hat{u}_t t + \hat{u}_{tt} t^2 + \hat{u}_{xt} x t$$

Similarly, we wish to obtain a space-time representation of the fluxes: (the fluxes don't need to be saved, so they don't take up storage)

$$f(x, t) = \hat{f}_0 + \hat{f}_x x + \hat{f}_{xx} \left( x^2 - \frac{1}{12} \right) + \hat{f}_t t + \hat{f}_{tt} t^2 + \hat{f}_{xt} x t$$

We start the iteration with :  $\hat{u}_t = \hat{u}_{tt} = \hat{u}_{xt} = 0$  and  $\hat{f}_t = \hat{f}_{tt} = \hat{f}_{xt} = 0$

V. Imp. Questions: 1) Given approx.  $u(x,t)$ , how to obtain improved  $f(x,t)$ ?

2) How to obtain an improved space-time representation? i.e.  $\hat{u}_t$ ,  $\hat{u}_{tt}$  and  $\hat{u}_{xt}$

STEP II) Pick a space-time element. Pick a set of *nodal points* in a *space-time element*. 1d shown here; has been extended to multi-d.

$u(x_i, t_i)$  can be evaluated at each such nodal point “ $i = 4, 5, 6$ ”.

STEP III) Use nodal values to find nodal fluxes  $f_i = f(u(x_i, t_i))$ .

STEP IV) Obtain modal representation of fluxes:

Notice: *Finite Difference-like forms*

$$\hat{f}_0 = (4f_1 + f_2 + f_3)/6 \quad ;$$

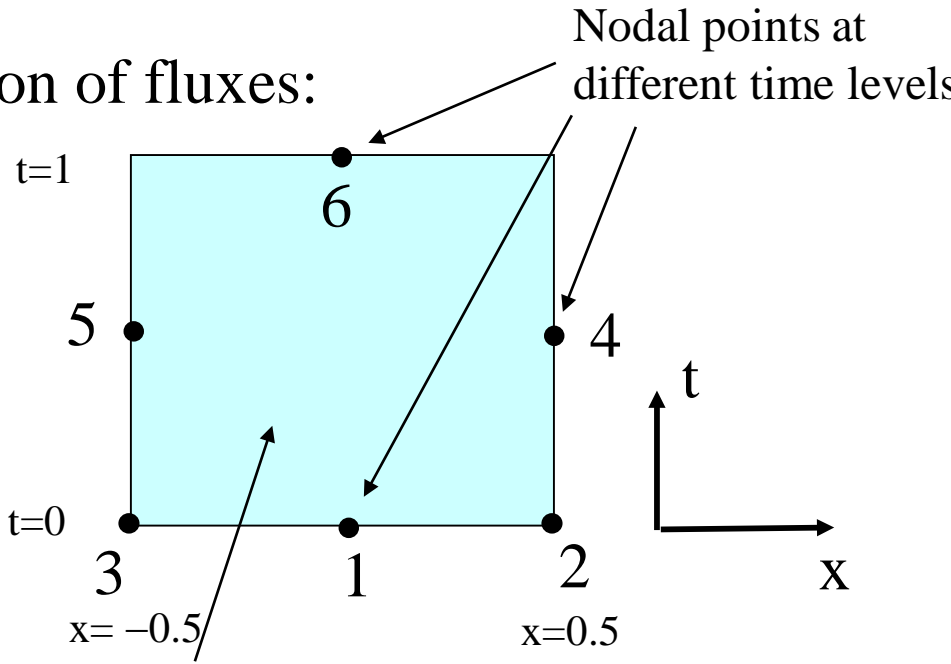
$$\hat{f}_x = (f_2 - f_3) \quad ;$$

$$\hat{f}_{xx} = 2(f_2 - 2f_1 + f_3) \quad ;$$

$$\hat{f}_t = f_1 - 2f_2 - 2f_3 + 2f_4 + 2f_5 - f_6 \quad ;$$

$$\hat{f}_{tt} = -2(f_1 - f_2 - f_3 + f_4 + f_5 - f_6) \quad ;$$

$$\hat{f}_{xt} = -2(f_2 - f_3 - f_4 + f_5)$$



Space-time element in (x,t)  
Spans [-.5,.5]x[0,1]

Notice:  $t=0$  variables only evaluated once; saves float pts.

STEP V) Use space-time basis functions as *test functions* to derive update equations:

$$\phi_1(x,t) = t \quad ; \quad \phi_2(x,t) = t^2 \quad ; \quad \phi_3(x,t) = x t$$

Make Galerkin, i.e. **weak-form integration over the space-time element** :-

$$\partial_t u(x,t) + \partial_x f(x,t) = 0$$

$$f(x,t) = \hat{f}_0 + \hat{f}_x x + \hat{f}_{xx} \left( x^2 - \frac{1}{12} \right) + \hat{f}_t t + \hat{f}_{tt} t^2 + \hat{f}_{xt} x t$$

$$u(x,t) = \hat{w}_0 + \hat{w}_x x + \hat{w}_{xx} \left( x^2 - \frac{1}{12} \right) + \hat{u}_t t + \hat{u}_{tt} t^2 + \hat{u}_{xt} x t$$

Galerkin formulation:

$$\iint_{x \in [-1/2, 1/2], t \in [0, 1]} \phi_i(x,t) \left[ \partial_t u(x,t) + \partial_x f(x,t) \right] dx dt = 0 \quad \text{for } i = 1, 2, 3$$

This gives us the *update equations*:-

(Notice that this is the part where we do **dynamics**, because we relate gradients of flux to the time-rate of change of the conserved variables!!!)

$$\hat{u}_t = -\hat{f}_x \quad ; \quad \hat{u}_{tt} = -\hat{f}_{xt}/2 \quad ; \quad \hat{u}_{xt} = -2\hat{f}_{xx}$$

Go back to STEP II and iterate!

For an  $N^{\text{th}}$  order scheme, even in multi-dimensions, this process can be shown to converge in  $(N-1)$  iterations. – **Picard Iteration**

**ADER can now be used in Predictor-Corrector fashion to obtain a *one-step update scheme* for conservation laws.**

**We've described the Predictor Step. Next, we describe efficient evaluation of the Corrector Step.**

## Flowchart for Initializing ADER-CG Iteration

Start with :  $u(x, t) = \hat{w}_0 + \hat{w}_x x + \hat{w}_{xx} \left( x^2 - \frac{1}{12} \right)$

$u(x_i, t_i=0)$  evaluated at each spatial nodal point “ $i = 1, \dots, 3$ ”.  
 $x_1 = -0.5$  ;  $x_2 = 0.0$  ;  $x_3 = 0.5$

Use nodal values,  $u(x_i, t_i)$  to find nodal fluxes  $f_i = f(u(x_i, t_i))$ ,  $i=1, \dots, 3$

Use nodal fluxes  $f_i$  to obtain modal fluxes  $\hat{f}_i$   
 $\hat{f}_0 = (4f_1 + f_2 + f_3)/6$  ;  $\hat{f}_x = (f_2 - f_3)$  ;  $\hat{f}_{xx} = 2(f_2 - 2f_1 + f_3)$

We start the iteration with :  $\hat{u}_t = \hat{u}_{tt} = \hat{u}_{xt} = 0$  and  $\hat{f}_t = \hat{f}_{tt} = \hat{f}_{xt} \stackrel{48}{=} 0$

## Flowchart for ADER-CG Iteration

Start with :  $u(x, t) = \hat{w}_0 + \hat{w}_x x + \hat{w}_{xx} \left( x^2 - \frac{1}{12} \right) + \hat{u}_t t + \hat{u}_{tt} t^2 + \hat{u}_{xt} x t$

$u(x_i, t_i)$  evaluated at each space-time nodal point “ $i = 4, 5, 6$ ”.  
 $(x_4, t_4) = (-.5, .5)$  ;  $(x_5, t_5) = (0.5, 0.5)$  ;  $(x_6, t_6) = (0, 1)$

Use nodal values,  $u(x_i, t_i)$  to find space-time nodal fluxes  $f_i = f(u(x_i, t_i))$

Use nodal fluxes  $f_i$  to obtain modal fluxes  $\hat{f}_i$  :  $\hat{f}_t = f_1 - 2f_2 - 2f_3 + 2f_4 + 2f_5 - f_6$  ;  
 $\hat{f}_{tt} = -2(f_1 - f_2 - f_3 + f_4 + f_5 - f_6)$  ;  $\hat{f}_{xt} = -2(f_2 - f_3 - f_4 + f_5)$

Update equations :  $\hat{u}_t = -\hat{f}_x$  ;  $\hat{u}_{tt} = -\hat{f}_{xt}/2$  ;  $\hat{u}_{xt} = -2\hat{f}_{xx}$

N-1 iterations for an N<sup>th</sup> order scheme.

## 1D ADER Corrector: Rapid strategy for obtaining numerical fluxes

Dumbser, Kaser & Toro (2008), Balsara et al. (2009), Balsara et al. (2013)

Say for the governing equation :  $\partial_t u + \partial_x f(u) = 0$

We have obtained the space-time representation of “u” and “f”,  
i.e. within *each* zone we have:

$$u(x, t) = \hat{w}_0 + \hat{w}_x x + \hat{w}_{xx} \left( x^2 - \frac{1}{12} \right) + \hat{u}_t t + \hat{u}_{tt} t^2 + \hat{u}_{xt} x t$$

$$f(x, t) = \hat{f}_0 + \hat{f}_x x + \hat{f}_{xx} \left( x^2 - \frac{1}{12} \right) + \hat{f}_t t + \hat{f}_{tt} t^2 + \hat{f}_{xt} x t$$

Question: How do we rapidly obtain the numerical flux after we have obtained the space-time representation?

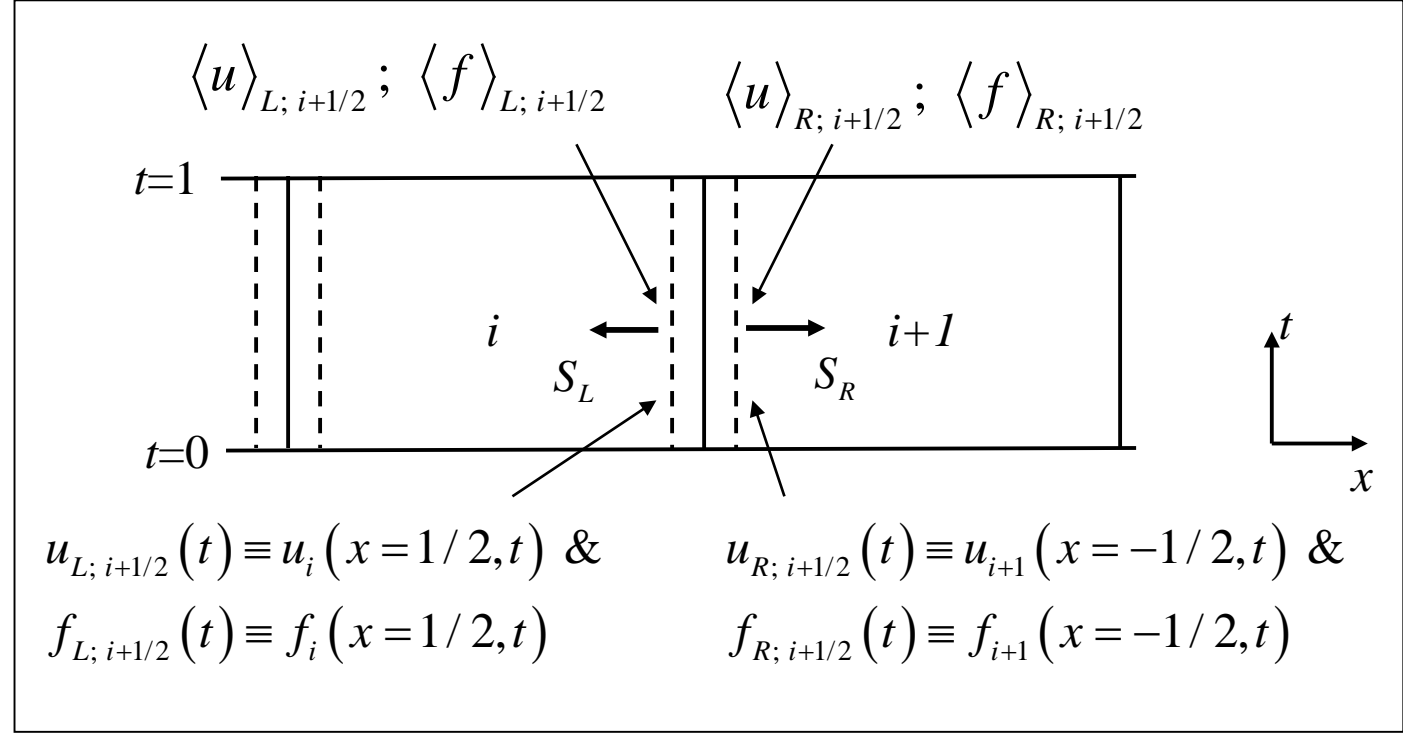
Define:

$$\langle f \rangle_{L; i+1/2} \equiv \int_{t=0}^1 f_{L; i+1/2}(t) dt ;$$

$$\langle f \rangle_{R; i+1/2} \equiv \int_{t=0}^1 f_{R; i+1/2}(t) dt ;$$

$$\langle u \rangle_{L; i+1/2} \equiv \int_{t=0}^1 u_{L; i+1/2}(t) dt ;$$

$$\langle u \rangle_{R; i+1/2} \equiv \int_{t=0}^1 u_{R; i+1/2}(t) dt ;$$



Consider the v. simple case of the HLL flux:

$$f_{i+1/2}^{HLL}(t) = \left[ \frac{S_R}{S_R - S_L} \right] f_{L; i+1/2}(t) - \left[ \frac{S_L}{S_R - S_L} \right] f_{R; i+1/2}(t) + \left[ \frac{S_R S_L}{S_R - S_L} \right] (u_{R; i+1/2}(t) - u_{L; i+1/2}(t))$$

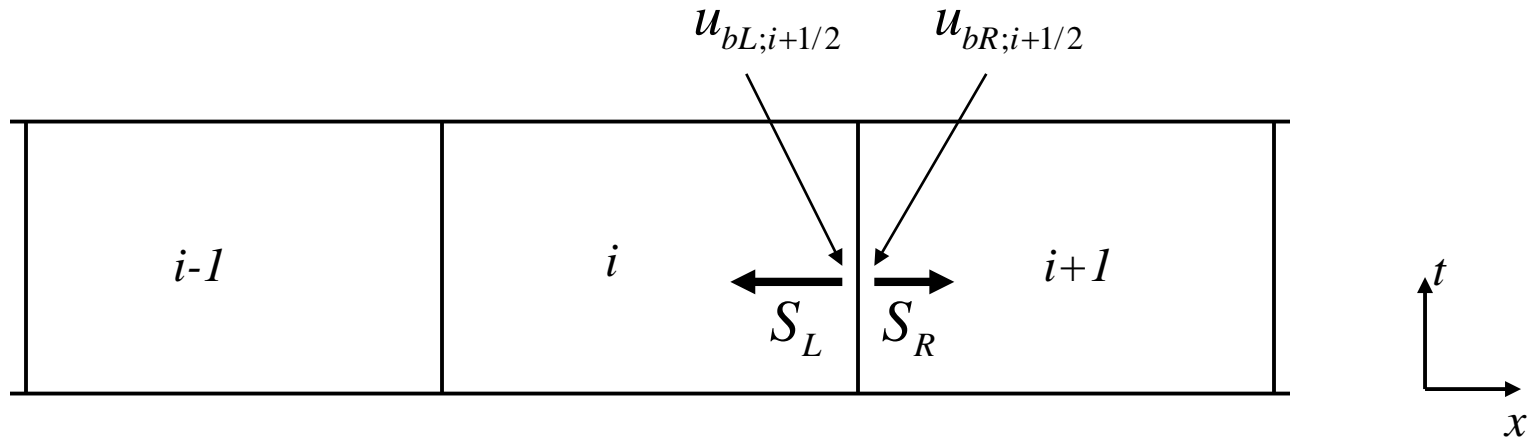
The numerical flux is then given by :  $\langle f \rangle_{i+1/2}^{HLL} \equiv \int_{t=0}^1 f_{i+1/2}^{HLL}(t) dt$

If we freeze  $\lambda_L$  and  $\lambda_R$  in some intelligent way (described later) then we can write:

$$\langle f \rangle_{i+1/2}^{HLL} \equiv \left[ \frac{S_R}{S_R - S_L} \right] \langle f \rangle_{L; i+1/2} - \left[ \frac{S_L}{S_R - S_L} \right] \langle f \rangle_{R; i+1/2} + \left[ \frac{S_R S_L}{S_R - S_L} \right] (\langle u \rangle_{R; i+1/2} - \langle u \rangle_{L; i+1/2})$$

Above example showed how time-averaging can be done. For multidimensional problems, the averaging can be done in space & time. Can also be done for other Riemann solvers.

Question: How does one obtain  $S_L$  and  $S_R$  ?



$$u_{bL; i+1/2} \equiv u_i \left( x = 1/2, t = 1/2 \right) \text{ and } u_{bR; i+1/2} \equiv u_{i+1} \left( x = -1/2, t = 1/2 \right)$$

are honest to goodness physical states at the space-time barycenters of the faces.

They can be used to obtain  $\lambda_L$  and  $\lambda_R$

*These ideas extend to multidimensions; they can also be used to yield the electric fields for MHD.*

## 7.5.2.1) Multidimensional ADER-CG Predictor Step

Within a zone we start with the third order spatial reconstruction:

$$U_{i,j}(\tilde{x}, \tilde{y}, \tilde{t}) = \bar{U}_{i,j} + \hat{U}_{i,j;x} \tilde{x} + \hat{U}_{i,j;y} \tilde{y} + \hat{U}_{i,j;xx} \left( \tilde{x}^2 - \frac{1}{12} \right) + \hat{U}_{i,j;yy} \left( \tilde{y}^2 - \frac{1}{12} \right) + \hat{U}_{i,j;xy} \tilde{x} \tilde{y}$$

To endow time-dependence within the zone, we want (Zero new terms to begin with):

$$U_{i,j}(\tilde{x}, \tilde{y}, \tilde{t}) = \bar{U}_{i,j} + \hat{U}_{i,j;x} \tilde{x} + \hat{U}_{i,j;y} \tilde{y} + \hat{U}_{i,j;xx} \left( \tilde{x}^2 - \frac{1}{12} \right) + \hat{U}_{i,j;yy} \left( \tilde{y}^2 - \frac{1}{12} \right) + \hat{U}_{i,j;xy} \tilde{x} \tilde{y} \\ + \hat{U}_{i,j;t} \tilde{t} + \hat{U}_{i,j;tt} \tilde{t}^2 + \hat{U}_{i,j;xt} \tilde{x} \tilde{t} + \hat{U}_{i,j;yt} \tilde{y} \tilde{t}$$

Question: Why do we add just these terms? (Hint: Think Taylor series)

Recall that we needed the gradients of the x- and y- fluxes to obtain the predictor step. Same holds true here. So let us write the space-time moments of the x- and y-fluxes:

$$F_{i,j}(\tilde{x}, \tilde{y}, \tilde{t}) = \hat{F}_{i,j} + \hat{F}_{i,j;x} \tilde{x} + \hat{F}_{i,j;y} \tilde{y} + \hat{F}_{i,j;xx} \left( \tilde{x}^2 - \frac{1}{12} \right) + \hat{F}_{i,j;yy} \left( \tilde{y}^2 - \frac{1}{12} \right) + \hat{F}_{i,j;xy} \tilde{x} \tilde{y} \\ + \hat{F}_{i,j;t} \tilde{t} + \hat{F}_{i,j;tt} \tilde{t}^2 + \hat{F}_{i,j;xt} \tilde{x} \tilde{t} + \hat{F}_{i,j;yt} \tilde{y} \tilde{t}$$

$$G_{i,j}(\tilde{x}, \tilde{y}, \tilde{t}) = \hat{G}_{i,j} + \hat{G}_{i,j;x} \tilde{x} + \hat{G}_{i,j;y} \tilde{y} + \hat{G}_{i,j;xx} \left( \tilde{x}^2 - \frac{1}{12} \right) + \hat{G}_{i,j;yy} \left( \tilde{y}^2 - \frac{1}{12} \right) + \hat{G}_{i,j;xy} \tilde{x} \tilde{y} \\ + \hat{G}_{i,j;t} \tilde{t} + \hat{G}_{i,j;tt} \tilde{t}^2 + \hat{G}_{i,j;xt} \tilde{x} \tilde{t} + \hat{G}_{i,j;yt} \tilde{y} \tilde{t}$$

Question: How would you obtain the spatial moments of the fluxes?

What about temporal moments?

How do we relate the moments of the fluxes to the moments of  $U_{i,j}(\tilde{x}, \tilde{y}, \tilde{t})$ ?

Governing equation: 
$$\frac{\partial U_{i,j}(\tilde{x}, \tilde{y}, \tilde{t})}{\partial \tilde{t}} + \frac{\Delta t}{\Delta x} \frac{\partial F_{i,j}(\tilde{x}, \tilde{y}, \tilde{t})}{\partial \tilde{x}} + \frac{\Delta t}{\Delta y} \frac{\partial G_{i,j}(\tilde{x}, \tilde{y}, \tilde{t})}{\partial \tilde{y}} = 0$$

Galerkin Projection with a test function  $\phi(\tilde{x}, \tilde{y}, \tilde{t})$ :

$$\int_{\tilde{x}=-1/2}^{\tilde{x}=1/2} \int_{\tilde{y}=-1/2}^{\tilde{y}=1/2} \int_{\tilde{t}=0}^{\tilde{t}=1} \phi(\tilde{x}, \tilde{y}, \tilde{t}) \left[ \frac{\partial U_{i,j}(\tilde{x}, \tilde{y}, \tilde{t})}{\partial \tilde{t}} + \frac{\Delta t}{\Delta x} \frac{\partial F_{i,j}(\tilde{x}, \tilde{y}, \tilde{t})}{\partial \tilde{x}} + \frac{\Delta t}{\Delta y} \frac{\partial G_{i,j}(\tilde{x}, \tilde{y}, \tilde{t})}{\partial \tilde{y}} \right] d\tilde{x} d\tilde{y} d\tilde{t} = 0$$

To understand how it goes, let us explicitly try out  $\phi(\tilde{x}, \tilde{y}, \tilde{t}) = \tilde{t}$ . Show that we get:

$$\hat{U}_{i,j;t} + \frac{4}{3} \hat{U}_{i,j;tt} = - \hat{F}_{i,j;x} - \hat{G}_{i,j;y} - \frac{2}{3} \hat{F}_{i,j;xt} - \frac{2}{3} \hat{G}_{i,j;yt}$$

Similarly, with  $\phi(\tilde{x}, \tilde{y}, \tilde{t}) = \tilde{t}^2$  :

$$\hat{U}_{i,j;t} + \frac{3}{2} \hat{U}_{i,j;tt} = - \hat{F}_{i,j;x} - \hat{G}_{i,j;y} - \frac{3}{4} \hat{F}_{i,j;xt} - \frac{3}{4} \hat{G}_{i,j;yt}$$

Similarly, with  $\phi(\tilde{x}, \tilde{y}, \tilde{t}) = \tilde{x} \tilde{t}$  :  $\hat{U}_{i,j;xt} = - 2 \hat{F}_{i,j;xx} - \hat{G}_{i,j;xy}$

Similarly, with  $\phi(\tilde{x}, \tilde{y}, \tilde{t}) = \tilde{y} \tilde{t}$  :  $\hat{U}_{i,j;yt} = - \hat{F}_{i,j;xy} - 2 \hat{G}_{i,j;yy}$

Recall that this is a finite element-like procedure.

We can resort to iterative improvement of the

moments :  $\hat{U}_{i,j;t}$  ,  $\hat{U}_{i,j;tt}$  ,  $\hat{U}_{i,j;xt}$  and  $\hat{U}_{i,j;yt}$  .

Question: How would such an iteration work? Answer: Break it into two parts & see.

It turns out that, at third order, the process converges in two iterations!

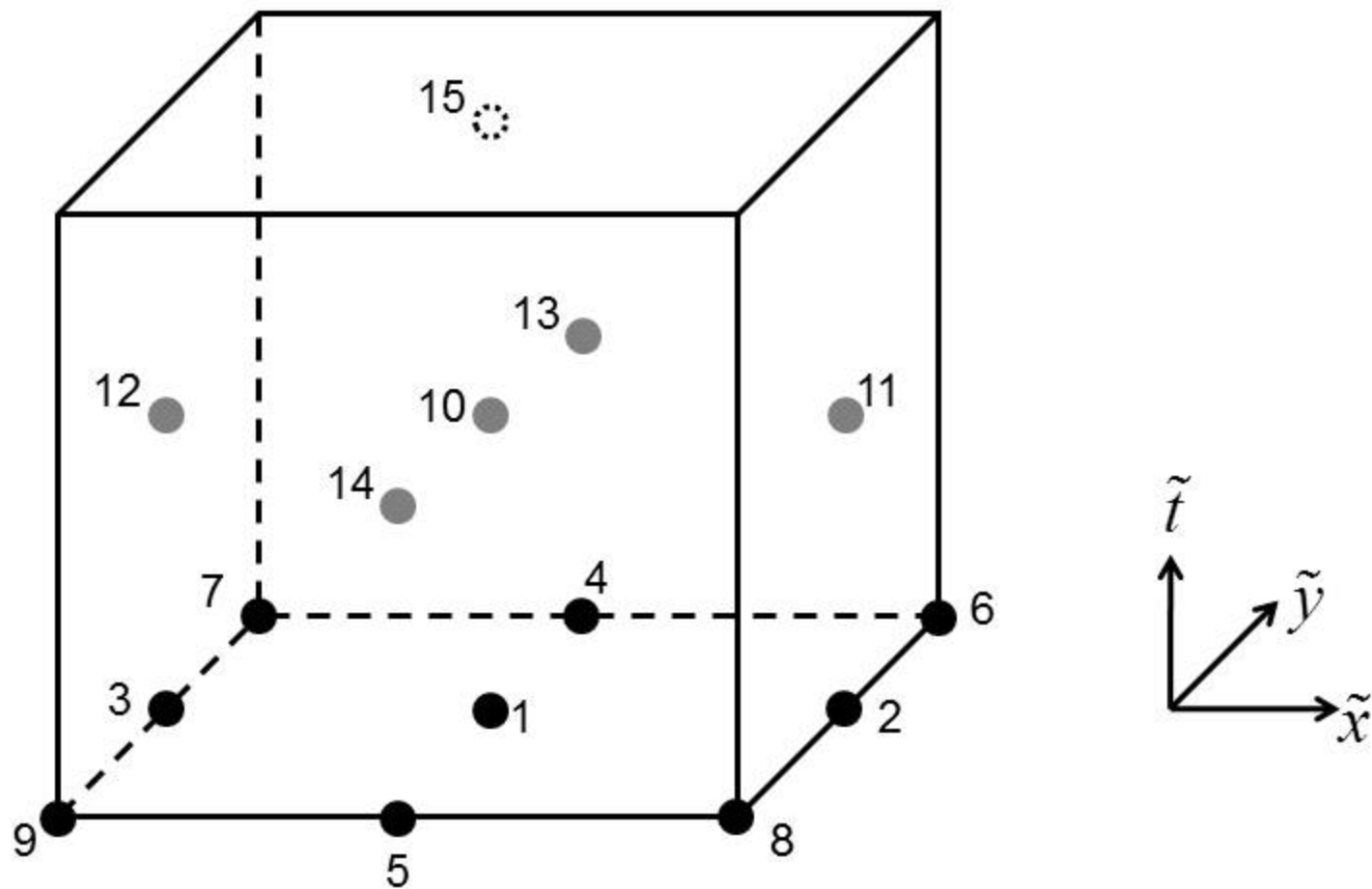


*Fig. 7.9 shows the placement of nodal points in space and time. The origin of our local coordinate system is actually centered at the first nodal point. The nine black circles, labeled 1 to 9, correspond to the nodes at time = 0. The five grey circles, labeled 10 to 14, correspond to the nodes at time = 1/2. Node 10 is collocated at the center of the space-time cube. Nodes 11 and 12 are centered in the x-faces; nodes 13 and 14 are centered in the y-faces. The dashed circle corresponds to the node 15 at time = 1. It is collocated at the center of the top face of the space-time cube.*

From the spatial nodal points (Only evaluated *once* at the start of the iteration.):

$$\{(0,0,0), (1/2,0,0), (-1/2,0,0), (0,1/2,0), (0,-1/2,0), \\ (1/2,1/2,0), (-1/2,1/2,0), (1/2,-1/2,0), (-1/2,-1/2,0)\}$$

We get:

$$\hat{F}_{i,j;xx} = 2(F_{i,j}^2 - 2F_{i,j}^1 + F_{i,j}^3) \quad ; \quad \hat{F}_{i,j;yy} = 2(F_{i,j}^4 - 2F_{i,j}^1 + F_{i,j}^5) \quad ;$$

$$\hat{F}_{i,j;xy} = F_{i,j}^6 - F_{i,j}^7 - F_{i,j}^8 + F_{i,j}^9 \quad ;$$

$$\hat{F}_{i,j;x} = F_{i,j}^2 - F_{i,j}^3 \quad ; \quad \hat{F}_{i,j;y} = F_{i,j}^4 - F_{i,j}^5 \quad ; \quad \hat{F}_{i,j} = F_{i,j}^1 + (\hat{F}_{i,j;xx} + \hat{F}_{i,j;yy})/12$$

Notice the finite difference-like forms!

From the space-time nodal points (Evaluated for *each* iteration):

$$\{(0,0,1/2), (1/2,0,1/2), (-1/2,0,1/2), (0,1/2,1/2), (0,-1/2,1/2), (0,0,1)\}$$

We get:

$$\hat{F}_{i,j;xt} = 2(F_{i,j}^{11} - F_{i,j}^{12} - F_{i,j}^2 + F_{i,j}^3) \quad ; \quad \hat{F}_{i,j;yt} = 2(F_{i,j}^{13} - F_{i,j}^{14} - F_{i,j}^4 + F_{i,j}^5) \quad ;$$

$$\hat{F}_{i,j;tt} = 2(F_{i,j}^{15} - 2F_{i,j}^{10} + F_{i,j}^1) \quad ; \quad \hat{F}_{i,j;t} = F_{i,j}^{15} - F_{i,j}^1 - \hat{F}_{i,j;tt}$$

## 7.5.2.2) Multidimensional ADER-CG Corrector Step

The construction from the previous sub-section has given us the space and time representation of the conserved variables and the fluxes.

We wish to obtain the numerical flux in a **quadrature-free** fashion. In doing so, we wish to use all the space-time information that we have generated.

$$\begin{aligned} F_{i+1/2,j}(\tilde{y}, \tilde{t}) &= \left[ \frac{S_R}{S_R - S_L} \right] F_{L; i+1/2,j}(\tilde{y}, \tilde{t}) - \left[ \frac{S_L}{S_R - S_L} \right] F_{R; i+1/2,j}(\tilde{y}, \tilde{t}) \\ &\quad + \left[ \frac{S_R S_L}{S_R - S_L} \right] \left( U_{R; i+1/2,j}(\tilde{y}, \tilde{t}) - U_{L; i+1/2,j}(\tilde{y}, \tilde{t}) \right) \end{aligned}$$

The extremal speeds,  $S_L$  and  $S_R$ , are obtained from:

$$U_{L; i+1/2,j}^{(c)} = U_{i,j}(\tilde{x} = 1/2, \tilde{y} = 0, \tilde{t} = 1/2) \quad ; \quad U_{R; i+1/2,j}^{(c)} = U_{i+1,j}(\tilde{x} = -1/2, \tilde{y} = 0, \tilde{t} = 1/2)$$

As before, we freeze these speeds. Question: What does this buy us?



$$\int_{\tilde{t}=0}^{\tilde{t}=1} \int_{\tilde{y}=-1/2}^{\tilde{y}=1/2} \mathbf{U}_{L; i+1/2, j}(\tilde{y}, \tilde{t}) d\tilde{y} d\tilde{t} = \left( \bar{\mathbf{U}}_{i, j} + \frac{1}{2} \hat{\mathbf{U}}_{i, j; x} + \frac{1}{6} \hat{\mathbf{U}}_{i, j; xx} \right) + \frac{1}{2} \left( \hat{\mathbf{U}}_{i, j; t} + \frac{1}{2} \hat{\mathbf{U}}_{i, j; xt} \right) + \frac{1}{3} \hat{\mathbf{U}}_{i, j; tt}$$

Do analogously for  $\mathbf{F}_{L; i+1/2, j}(\tilde{y}, \tilde{t})$ .

$$\int_{\tilde{t}=0}^{\tilde{t}=1} \int_{\tilde{y}=-1/2}^{\tilde{y}=1/2} \mathbf{U}_{R; i+1/2, j}(\tilde{y}, \tilde{t}) d\tilde{y} d\tilde{t} = \left( \bar{\mathbf{U}}_{i+1, j} - \frac{1}{2} \hat{\mathbf{U}}_{i+1, j; x} + \frac{1}{6} \hat{\mathbf{U}}_{i+1, j; xx} \right) + \frac{1}{2} \left( \hat{\mathbf{U}}_{i+1, j; t} - \frac{1}{2} \hat{\mathbf{U}}_{i+1, j; xt} \right) + \frac{1}{3} \hat{\mathbf{U}}_{i+1, j; tt}$$

Do analogously for  $\mathbf{F}_{R; i+1/2, j}(\tilde{y}, \tilde{t})$ .

## 7.8) Numerical Tests for Euler Flow

### 7.8.1) Demonstrating Accuracy on Multidimensional Test Problems

We study scheme performance for vortex flow with increasing resolution.

Questions: On a coarse mesh, with just a few zones across, which scheme performs better? As the mesh is refined, which scheme performs better? How do you measure order of accuracy?

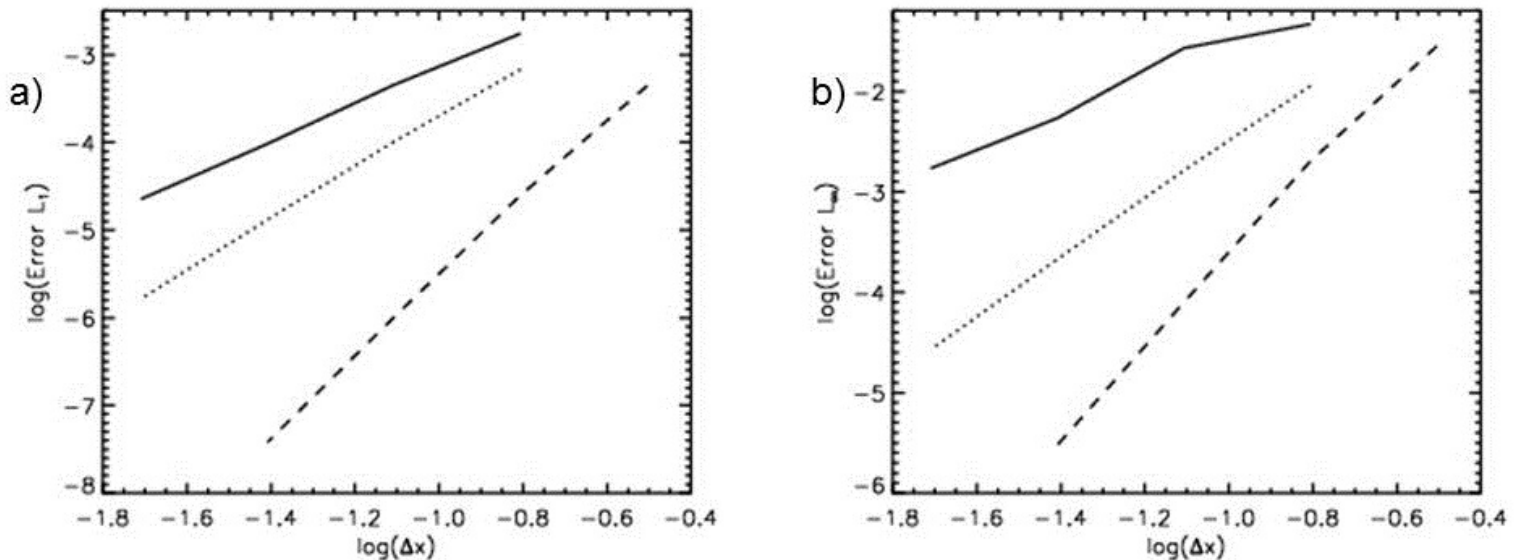
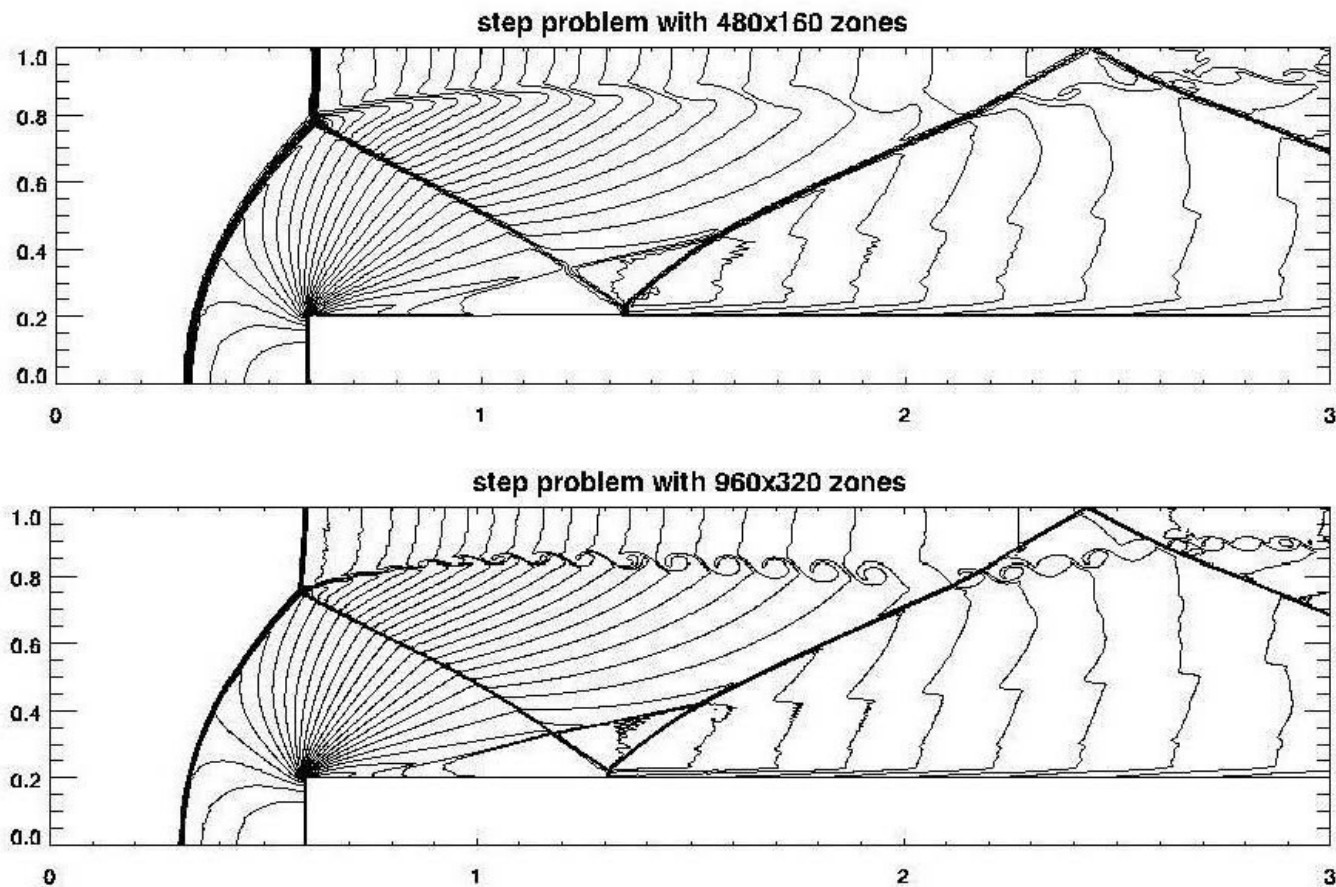


Fig. 7.10 shows the variation of the  $L_1$  (left panel) and  $L_\infty$  (right panel) errors as a function of zone size for the 2d vortex problem. The solid lines show the second order predictor-corrector scheme with minmod limiter; the dotted and dashed lines show third and fourth order ADER-WENO schemes respectively.

## 5.8.2) Forward Facing Step Test Problem



*Fig. 7.11 shows the density variable from the forward facing step problem at resolutions of 480X160 and 960X320 zones at a time of 4 units. Thirty equally spaced contours are shown in the density variable ranging from 0.105 to 6.699. The fourth order scheme with a linearized Riemann solver was used. We see the beginnings of the vortex sheet roll-up at a resolution of 480X160 zones and the 960X320 zone simulation captures the roll-up very clearly.*

## 7.8.3) Double Mach Reflection Problem

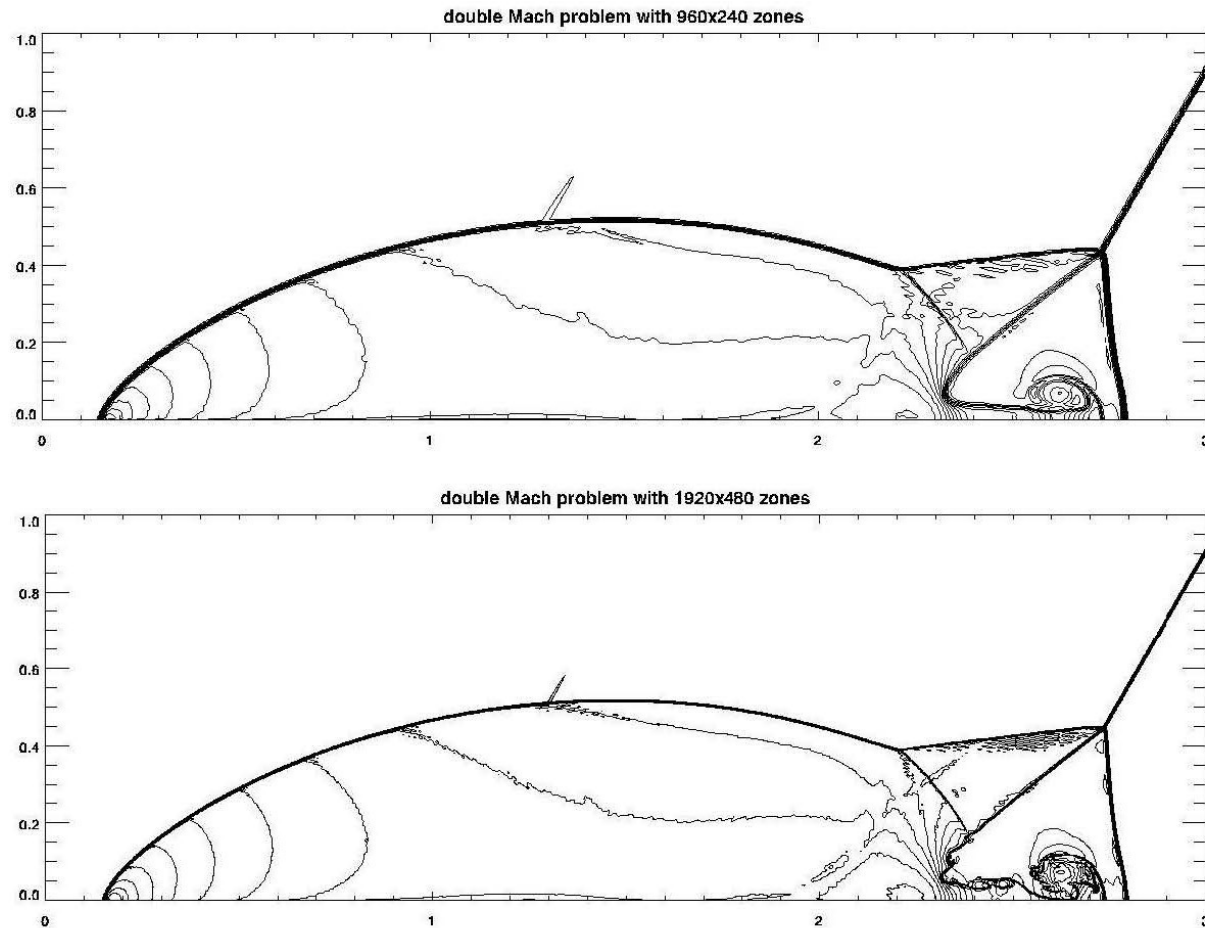


*Fig. 7.12 shows a resolution study of the double Mach reflection of a strong shock. The top and bottom panels show the density from 960X240 and 1920X480 zone simulations. The 4<sup>rd</sup> order ADER-WENO scheme with a linearized Riemann solver was used. 30 contours were fit between a range of 1.4 and 20.975. We clearly see the roll up of the Mach stem due to Kelvin-Helmholtz instability in the higher resolution simulation.*